

**Numerical Study of MHD Heat and Mass Transfer Flow Past an Infinite Vertical Porous Plate with Thermal Conductivity and Soret Effect in the Presence of Suction or Injection.**

by

Md. Mahmudul Hasan

Roll No. 1451556

A thesis submitted in partial fulfillment of the requirements for the degree of Master of Science in Mathematics



Khulna University of Engineering & Technology

Khulna-9203, Bangladesh

June 2016

## Declaration

This is to certify that the thesis work entitled “**Numerical Study of MHD Heat and Mass Transfer Flow Past an Infinite Vertical Porous Plate with Thermal Conductivity and Soret Effect in the Presence of Suction or Injection**” has been carried out by Md. Mahmudul Hasan in the Department of Mathematics, Khulna University of Engineering & Technology, Khulna, Bangladesh. The above thesis work or any part of this work has not been submitted anywhere for the award of any degree or diploma.

Signature of Supervisor

Signature of Student



## Acknowledgements

First and foremost, praises and thanks to Allah, the Almighty for His showers of blessings throughout my research work to complete the thesis successfully.

I would like to express my sincere gratitude to my supervisor Dr. M. M. Touhid Hossain, Professor, Department of Mathematics, Khulna University of Engineering & Technology (KUET), Khulna, for his invaluable guidance and encouragement throughout the research. His continued support led me to the right way.

I am deeply grateful to Mr. Tanvir Ahmed, PhD candidate at the University of Newcastle, Australia, for his generous and timely help as well as for many discussions carried out from long distance via email that helped me sort out the technical details of my work.

I would like to extend my thanks to the Department of Mathematics, KUET for providing me all kinds of support and help from the Department. My sense of gratitude to all of my respected teachers of the Department of Mathematics, KUET for their cordial help and valuable suggestions.

It is not possible to express in words my sincere indebtedness to my brother Dr. Md. Mezbaur Bahar for his continuous cooperation and inspiration during the preparation of this thesis. Finally, I express my deepest gratitude to my parents for whom I am able to see the beautiful sights and sound of the world.

## **Abstract**

In the present study, numerical investigations have been performed to examine the MHD mixed convection boundary layer flow over an impulsively started vertical permeable plate with thermal-diffusion (Soret) and diffusion-thermo (Dufour) effects. Under some simplified assumptions and using usual Boussinesq approximation, the governing boundary layer partial differential equations have been transformed first into a non-dimensional system of non-linear coupled partial differential equations by introducing suitable transformations. Secondly, the transformed set of partial differential equations has been solved numerically using the implicit finite difference numerical method. Numerical solutions are obtained for the velocity and temperature fields as well as the concentration distribution for different values of the physical parameters entering into the problem. The effects of these various involved parameters on the velocity and temperature fields and on the concentration distribution have been investigated. Finally, the obtained results involving the effects of these physical parameters on the flow phenomena have been discussed with the help of graphs. The numerical results have shown that the above mentioned effects have to be taken into consideration in the flow field and in the heat and mass transfer process. It is also expected that the finding of this investigation may be useful for the study of power engineering, geothermal and geophysical process.

# Contents

	Page
Title Page	i
Declaration	ii
Approval	iii
Acknowledgements	iv
Abstract	v
Contents	vi
List of Figures	viii
<b>Chapter I</b> Introduction	1
1.1 Literature Review	
1.2 Some Available information on MHD	
1.2.1 Magnetohydrodynamics (MHD)	4
1.2.2 MHD Boundary Layer Phenomena	6
1.2.3 Mass Transfer	7
1.2.4 MHD and Heat Transfer	7
1.2.5 Mixed Convection	8
1.2.6 Heat and Mass Transfer	9
1.3 Useful Dimensionless Parameters	10
<b>Chapter II</b> Governing Equations	13
2.1 Basic Governing Equations	13
<b>Chapter III</b> Calculation Technique	22
3.1 Finite Difference Method	22
<b>Chapter IV</b> Finite Difference Solution of MHD Mixed Convection Flow through an Impulsively Stretched Permeable Vertical Plate with Thermal-Diffusion and Diffusion-Thermo Effects	26
4.1 Mathematical Model of the Flow	26
4.2 Mathematical Formulation	28

4.3 Numerical Solution	30
4.4 Results and Discussion	32
<b>Chapter V</b> Conclusions	52
References	54
Nomenclature	57

## LIST OF FIGURES

Figure No	Description	Page
Figure 2.1	Physical configuration and coordinate system	18
Figure 3.1	Space-Time index notation	23
Figure. 4.3.1	Implicit finite difference system grid	30
Figure 4.1	Velocity profiles for various values of dimensionless time, $\dagger$ .	32
Figure 4.2	Areas vs. dimensionless time, $\dagger$ .	33
Figure 4.3	Velocity profiles for various values of Grashof Number, $Gr$ .	34
Figure 4.4	Temperature profiles for various values of Grashof Number, $Gr$ .	35
Figure 4.5	Concentration profiles for various values of Grashof Number, $Gr$ .	35
Figure 4.6	Velocity profiles for various values of Modified Grashof Number, $Gm$ .	36
Figure 4.7	Temperature profiles for various values of Modified Grashof Number, $Gm$ .	36
Figure 4.8	Concentration profiles for various values of Modified Grashof Number, $Gm$ .	37
Figure 4.9	Velocity profiles for various values of Prandtl Number, $Pr$ .	37
Figure 4.10	Temperature profiles for various values of Prandtl Number, $Pr$ .	38
Figure 4.11	Concentration profiles for various values of Prandtl Number, $Pr$ .	38
Figure 4.12	Velocity profiles for various values of Dufour Number, $Du$ .	39
Figure 4.13	Temperature profiles for various values of Dufour Number, $Du$ .	39
Figure 4.14	Concentration profiles for various values of Dufour Number, $Du$ .	40
Figure 4.15	Velocity profiles for various values of Schmidt Number, $Sc$ .	40
Figure 4.16	Temperature profiles for various values of Schmidt Number, $Sc$ .	41
Figure 4.17	Concentration profiles for various values of Schmidt Number, $Sc$ .	41
Figure 4.18	Velocity profiles for various values of Soret Number, $Sr$ .	42
Figure 4.19	Temperature profiles for various values of Soret Number, $Sr$ .	42



Figure 4.20	Concentration profiles for various values of Soret Number, $Sr$ .	43
Figure 4.21	Velocity profiles for various values of Magnetic Parameter, $M$ .	44
Figure 4.22	Temperature profiles for various values of Magnetic Parameter, $M$ .	44
Figure 4.23	Concentration profiles for various values of Magnetic Parameter, $M$ .	45
Figure 4.24	Velocity profiles for various values of Permeability of the porous medium, $\chi$ .	45
Figure 4.25	Temperature profiles for various values of Permeability of the porous medium, $\chi$ .	46
Figure 4.26	Concentration profiles for various values of Permeability of the porous medium, $\chi$ .	46
Figure 4.27	Velocity profiles for various values of Suction Parameter, $\beta$ .	47
Figure 4.28	Temperature profiles for various values of Suction Parameter, $\beta$ .	47
Figure 4.29	Concentration profiles for various values of Suction Parameter, $\beta$ .	48
Figure 4.30	Velocity profiles for various values of Eckert Number, $Ec$ .	48
Figure 4.31	Temperature profiles for various values of Eckert Number, $Ec$ .	49
Figure 4.32	Concentration profiles for various values of Eckert Number, $Ec$ .	49
Figure 4.33	Velocity profiles for various values of Electrical conductivity, $\dagger$ .	50
Figure 4.34	Temperature profiles for various values of Electrical conductivity, $\dagger$ .	51
Figure 4.35	Concentration profiles for various values of Electrical conductivity, $\dagger$ .	51

## Nomenclature

$\sim$	Fluid viscosity
$k_1$	Permeability of the porous medium
$\epsilon$	Kinematic viscosity
$k_t$	Thermal diffusion ratio
$T_m$	Mean fluid temperature
$K_0$	Thermal conductivity of the ambient fluid
$S_T$	Thermal expansion coefficient
$S_C$	Concentration expansion coefficient
...	Density
$c_p$	Specific heat
}	Suction Parameter
$Gr$	Grashof Number
$Gm$	Modified Grashof Number
$U_0$	Uniform Plate velocity
$\kappa$	Permeability of the porous medium
$M$	Magnetic Parameter
$Sc$	Schmidt Number
$Sr$	Soret Number
$Pr$	Prandtl Number
$\dagger$	Vayriable thermal conductivity
$Du$	Dufour Number
$Ec$	Eckert Number
$D$	Coefficient of mass diffusivity

# CHAPTER I

## Introduction

### 1.1 Literature Review

The effect of thermal diffusion on MHD heat and mass transfer fluid flow past a continuously moving surface has a great importance to the engineering community and to the investigators in dealing with the problems related to many industrial processes and many technological fields. The free convection process involving the combined heat and mass transfer mechanism in a porous medium has been attracted considerable attention in the last decades, due to its much importance in industrial applications and in many engineering, geophysical and chemical engineering systems. In recent years, the study of free convective heat transfer flow along with mass transfer effects has become the object of extensive research due to its versatile applications in the design of steel rolling and nuclear power plants and in many engineering phenomenon such as rocket nozzles, cooling of nuclear reactors, high sinks in turbine blades, high speed aircrafts and their atmospheric re-entry, chemical devices and process equipment, cooling of electronic systems, thermal and insulating engineering, chemical catalytic reactors and filtration process in chemical engineering, aerodynamic heat shielding with transpiration cooling etc. The convection problem in porous medium has other applications in geothermal reservoirs and geothermal energy extractions. A comprehensive review of the studies of convective heat transfer mechanism through porous media has been made by Bejan *et al.* (2004), Inham *et al.* (2005), Vafai (2005), Nield and Bejan (2006) and so on. Moreover, considerable attention has been paid to the study of MHD heat and mass transfer flow because of the applications in geophysics, aeronautics and chemical engineering. Palani and Srikanth (2009) studied the MHD flow of an electrically conducting fluid over a semi-infinite vertical plate under the influence of the transversely applied magnetic field. Makinde (2010) investigated the MHD boundary layer flow with heat and mass transfer over a moving vertical plate in the presence of magnetic field and convective heat exchange at the surface. On the other hand, Duwairi (2005) analyzed viscous and Joule-heating effects on forced convection flow from radiative isothermal surfaces. The effect of viscous dissipation is usually characterized by the Eckert

number and has played a very important role in geophysical flow and in nuclear engineering that was studied by Alim *et al.* (2007). The effects of suction or injection on boundary layer flow also play an important role in various processes of engineering applications and have been widely investigated by numerous researchers. Various researchers have studied the effects of viscous dissipation and constant suction in different surface geometries. An analysis of two dimensional steady free convective flow of a conducting fluid in the presence of a magnetic field and a foreign mass past an infinite vertical porous and unmoving surface is carried out by Raptis (1983), when the heat flux is constant at the limiting surface and the magnetic Reynolds number of the flow is not small. Assuming constant suction at the surface, approximate solutions of the coupled nonlinear equations are derived for the velocity field, the temperature field, the magnetic field and for their related quantities. Agrawal *et al.* (1980) consider the steady laminar free convection flow with mass transfer of an electrically conducting liquid along a plane wall with periodic suction. Sattar (1993) analyzed the effect of free and forced convection boundary layer flow through a porous medium with large suction. The effect of similarity solution for MHD flow through vertical porous plate with suction have been studied by Mohammed *et al.* (2005). Mansour *et al.* (2008) described the influence of chemical reaction and viscous dissipation on MHD natural convection flow. Khaleque and Samad (2010) described the effects of radiation, heat generation, and viscous dissipation on MHD free convection flow along a stretching sheet.

Uwanta (2012) studied the effects of chemical reaction and radiation on heat and mass transfer flow past a semi-infinite vertical porous plate with constant mass flux and dissipation. Govardhan *et al.* (2012) presented a theoretical study on the influence of radiation on a steady free convection heat and mass transfer over an isothermal stretching sheet in the presence of a uniform magnetic field with viscous dissipation effect. Jai (2012) presented the study of a viscous dissipation and chemical reaction effects on flow past a stretching porous surface in a porous medium. In another article, a detailed numerical study on the combined effects of radiation and mass transfer on a steady MHD two-dimensional Marangoni convection flow over a flat surface in presence of joule-heating and viscous dissipation under influence of suction and injection is studied by Ibrahim (2013).

When heat and mass transfer occur simultaneously in a moving fluid affecting each other causes a cross diffusion effect, the mass transfer caused by temperature gradient is called the Soret effect, while the heat transfer caused by concentration effect is called the Dufour effect.

Soret and Dufour effects are important phenomena in areas such as hydrology, petrology and geosciences. The Soret effect, for instance, has been utilized for separation of isotope in a mixture between gases with very light molecular weight (He, H<sub>2</sub>) and of medium molecular weight (N<sub>2</sub>, air). The Dufour effect was recently found to be of order of considerable magnitude so that it cannot be neglected (Eckert and Drake (1974)). Many researchers studied Soret and Dufour effects; for example, Kafousias and Williaims (1995) examined Soret and Dufour effects on mixed free-forced convective and mass transfer boundary layer flow with temperature dependent viscosity. Uwanta *et al.* (2008) have analyzed MHD fluid flow over a vertical plate with Dufour and Soret effects. Postelnicu (2010) analyzed the effect of Soret and Dufour on heat and mass transfer. Later, Usman and Uwanta (2013) have considered the effect of thermal conductivity on MHD heat and mass transfer flow past an infinite vertical plate with Soret and Dufour effects. Recently, the effects of Soret and Dufour on an unsteady MHD free convection flow past a vertical porous plate in the presence of suction or injection have been investigated by Sarada and Shankar (2013). Most recently, using implicit finite difference scheme of Crank-Nicolson, Uwatana and Usman (2014) investigated the combined effects of Soret and Dufour on free convective heat and mass transfer on the unsteady boundary layer flow over a vertical channel in the presence of viscous dissipation and constant suction.

Hence our aim of this research is to extend the work of Usman and Uwanta (2013). The problem has been solved by finite difference method. The governing equations involved in this problem have been transformed into non-similar coupled partial differential equation by usual transformations. Finally, the results has been shown graphically.

The present thesis is composed of Five Chapters. An introduction including basic literature review, some available information on MHD and useful dimensionless parameters regarding our problem are presented in CHAPTER I.

Basic equations governing the problems with some simplifying assumptions are given in CHAPTER II. In CHAPTER III brief description of the Finite Difference calculation technique has been given. CHAPTER IV deals with the mathematical model of the problem with dimensional analysis. The numerical solution including the graphs and result and discussion have been given in this chapter. The conclusion gained from this research have been discussed in CHAPTER V.

## **1.2 Some Available Information on MHD**

### **1.2.1 Magnetohydrodynamics (MHD)**

Magnetohydrodynamics (MHD) is the study of the flow of electrically conducting fluids in electric and magnetic fields which is a branch of magneto fluid dynamics i.e. continuum mechanics. Probably the largest advance towards an understanding of such phenomena comes from the field of astrophysics. It has long been suspected that most of the matter in the universe is in the plasma or highly ionized gaseous state and much of the basic knowledge in the area of electromagnetic fluid dynamics evolved from these studies.

The field of MHD which consists of the study of a continuous, electrically conducting fluid under the influence of electromagnetic fields, is a branch of plasma physics. Originally, MHD included only the study of strictly incompressible fluid but today the terminology is applied to the study of partially ionized gases and therefore different names have been suggested, such as magneto-fluid-mechanics or magneto-aero-dynamics, but original nomenclature still persists. The essential requirement for problems to be analyzed under the laws of MHD is that the continuum approach be applicable.

There are many natural phenomena and engineering problems which are susceptible to MHD analysis. It is useful in astrophysics because much of the universe is filled with widely spaced charged particles and permeated through magnetic fields so that the continuum assumption becomes applicable. Geophysicists encounter MHD phenomena in the interactions of conducting fluids and magnetic fields that are present in and around heavenly bodies. Engineers employ MHD principles in the design of heat exchangers, pumps and flow meters, in space vehicle propulsion, control and re-entry problem, in designing communications and radar system, in creating novel power generating systems and in developing confinement schemes for controlled fusion.

The most important application of MHD is the generation of electrical power with the flow of an electrically conducting fluid through a transverse magnetic field. Recently, experiments with ionized gases have been performed with the aim of producing power on a large scale in stationary plants with large magnetic fields. Cryogenic and superconducting magnets are required to produce these very large magnetic fields. Generation of MHD power on a smaller

scale is of interest for space applications.

Generally it is known that, several intermediate transformations are necessary to convert the heat energy into electricity. Each of these steps involves a loss of energy. This naturally limits the overall efficiency, reliability and compactness of the conversion process. Methods for direct conversion to energy are now increasingly receiving attention. Of these, the fuel cell converts the chemical energy of fuel directly into electrical energy; fusion energy utilizes the energy released when two hydrogen nuclei fuse into a heavier one, and thermo electrical power generation uses a thermocouple. MHD power generation is another important new process that is receiving worldwide attention.

In the experiment of Faraday (1832), the principal MHD effects were first demonstrated. He discovered that a voltage was induced across the tube due to the motion of the mercury across the magnetic fields, perpendicular to the direction of flow and to the magnetic field by the experiment of the flow of mercury in glass tubes placed between poles of a magnet. He also suggested that electrical power could be generated in a load circuit by the interaction of a flowing conducting fluid and a magnetic field. Later, Alfven (1942) discovered MHD waves in the sun. These waves are produced by disturbances which propagate simultaneously in the conducting fluid and the magnetic field. The analogy that explains the generation of an Alfven wave is that of a harp string plucked while submerged in a fluid. The string provides elastic force and the fluid provides inertia force and they combine to propagate a perturbing wave through the fluid and the string.

In summary, MHD phenomena result from the mutual effect of a magnetic field and conducting fluid flowing across it. Thus an electromagnetic force is produced in a fluid flowing across a transverse magnetic field and the resulting current and magnetic field combine to produce a force that resists the fluid's motion. The current also generates its own magnetic field which distorts the original magnetic field. An opposing or pumping force on the fluid can be produced by applying an electric field perpendicularly to the magnetic field. Disturbance in either the magnetic field or the fluid can propagate in both (fields/directions?) to produce MHD waves as well as upstream and downstream wave phenomena. The science of MHD is the detailed study of these phenomena, which occur in nature and are produced in engineering devices.

### 1.2.2 MHD Boundary Layer Phenomena

Boundary layer phenomena occurs when the influence of a physical quantity is restricted to small regions near confining boundaries or when the viscous effect may be considered to be confined in a very thin layer to the boundaries or when the non-dimensional diffusion parameters such as the Reynolds number and the Peclet number or the magnetic Reynolds number are large. The boundary layers are then the velocity and thermal or magnetic boundary layers and each thickness is inversely proportional to the square root of the associated diffusion number.

From experimental flows, Prandtl observed that for large Reynolds number, the viscosity and thermal conductivity appreciably influenced the flow only near a wall and fathered classical fluid dynamic boundary layer theory. When distant measurements in the flow direction are compared with a characteristic dimension in that direction, transverse measurements compared with the boundary layer thickness and velocities compared with the free stream velocity then the Navier-Stokes and energy equations can be considerably simplified by neglecting small quantities. The number of component equations is reduced to those in the flow direction and pressure changes across the boundary layer are negligible. The pressure is then only a function of the flow direction and can be determined from the inviscid flow solution. Also the number of viscous term is reduced to the dominant term and the heat conduction in the flow direction is negligible.

The MHD boundary layer flows are separated into two types for considering the limiting cases of a very large or a negligible small magnetic Reynolds number. When the magnetic field is oriented in an arbitrary direction relative to a confining surface and the magnetic Reynolds number is very small, the flow direction component of the magnetic interaction and the corresponding Joule heating is only a function of the transverse magnetic field component and local velocity in the flow direction. Changes in the transverse magnetic field component and pressure across the boundary layer are negligible. The thickness of the magnetic boundary layer is very large and the induced magnetic field is negligible.

However, when the magnetic Reynolds number is very large, the magnetic boundary layer thickness is small and is of nearly the same size as the viscous and thermal boundary layers and then the MHD boundary layer equations must be solved simultaneously. In this case, the



magnetic field moves with the flow and is called frozen mass.

### **1.2.3 Mass Transfer**

Mass transfer problems are of importance in many processes and have therefore received a considerable amount of attention. In many mass transfer processes, heat transfer considerations arise owing to chemical reaction and are often due to the nature of the process. In processes such as drying, evaporation at the surface water body, energy transfer in a wet cooling tower and the flow in a desert cooler, heat and mass transfer occur simultaneously. In many of these processes, the interest lies in the determination of the total energy transfer, although in processes such as drying, the interest lies mainly in the overall mass transfer for moisture removal. Natural convection processes involving the combined mechanisms are also encountered in many natural processes, such as evaporation, condensation and agricultural drying, in many industrial applications involving solutions and mixtures in the absence of an externally induced flow and in many chemical processing systems. In many processes such as the curing of plastics, cleaning and chemical processing of materials relevant to the manufacture of printed circuitry, manufacture of pulp-insulated cables etc., the combined buoyancy mechanisms arise and the total energy and material transfer resulting from the combined mechanisms, has to be determined.

The basic heat and mass transfer problem is governed by the combined buoyancy effects rising from the simultaneous diffusion of thermal energy and of chemical species. Therefore the continuity, momentum, energy and concentration equations are coupled through the buoyancy terms alone, if the other effects, such as the Dufour effects are neglected. This would again be valid for low species concentration levels.

### **1.2.4 MHD and Heat Transfer**

With the advent of hypersonic flight, the field of MHD, as define above, which has attracted the interest of aero dynamists and associated largely with liquid metal pumping. It is possible to alter the flow and the heat transfer around high velocity vehicles provided that the air is sufficiently ionized. Furthermore, the invention of high temperature facilities such as the shock tube plasma jet has provided laboratory sources of following ionized gas, which provide an incentive for the study of plasma accelerators and generators. As a result of this, many of the classical problems of fluid mechanics have been reinvestigated. Some of these

analyses awake out of the natural tendency of scientists to search a new subject. In this case it was the academic problem of solving the equations of fluid mechanics with a new body force and another source of dissipation in the energy equation. Some time there were no practical applications for these results. As for example, natural convection MHD flows have been of interest to the engineering community only since the investigations directly applicable to the problems in geophysics and astrophysics. But it was in the field of aerodynamic heating that the largest interest was awakened.

The first paper on this subject was presented by Rossow (1957). His result for incompressible constant property flat plate boundary layer flow indicated that the skin friction and heat transfer were reduced substantially when a transverse magnetic field was applied to the fluid. This encouraged a multitude analysis for every imaginable type of aerodynamic flow and most of the research centered on the stagnation point, where in hypersonic flight, the highest degree of ionization could be expected. The result of these studies were sometimes contradictory concerning the amount by which the heat transfer would be reduced (some of this was due to misinterpretations and invalid comparison).

Eventually, however, it was concluded that the field strength, necessary to provide sufficient shielding against heat fluxes during atmospheric flight, were not competitive (in terms of weight) with other method of cooling (Sutton and Gloersen (1961)). However the invention of new light weight super conducting magnets has revived interests in the problem of providing heat projection during the very high velocity re-entry from orbital and super orbital flight (Levy and Petschek (1962)).

### **1.2.5 Mixed Convection**

Practically sometimes both the processes, natural and forced convection, are important and heat transfer is by mixed convection, in which neither mode is truly predominant. The main difference between the two really lies in the word external. A heated body lying on stagnant air loses energy by natural convection. But it also generates a buoyant flow above it and body placed on a moving air flow is subjected to an external flow and it becomes necessary to determine the natural, as well as the forced convection effects in the regime in which the heat transfer mechanisms lie.

When the study of MHD become a popular subject, it was normal that these flows would be

investigated with the additional ponder motive body force as well as the buoyancy force. At a first glance there seems to be no practical applications for these MHD solutions, for most heat exchangers utilize liquids, whose conductivity is so small that prohibitively large magnetic fields are necessary to influence the flow. But some nuclear power plants employ heat exchangers with liquid metal coolants, so the application of moderate magnetic fields to change the convection pattern appears feasible. Another classical natural convection problem is the thermal instability that occurs in a liquid heated from below. This subject is of natural interest to geophysicists and astrophysicists, although some applications might arise in boiling heat transfer.

The basic concepts involved in employing the boundary layer approximation to natural convection flows are very similar to those in forced flows. The main difference lies in the fact that pressure in the region beyond the boundary layer is hydrostatic instead of being imposed by an external flow and that the velocity outside the layer is zero. However the basic treatment and analysis remain the same, the book by Schlichting (1968) is an excellent collection of the boundary layer analysis. There are several methods for the solution of the boundary layer equations namely the similarity variable method, the perturbation method, analytical method, numerical method etc. and their details are available in the books written by Rosenberg (1969) and Patanker and Spalding (1970).

### **1.2.6 Heat and Mass Transfer**

Combined heat and mass transfer problems (Jaluria (1980)) are of importance in many processes and have therefore received a considerable amount of attention. In many mass transfer processes, heat transfer considerations arise owing to chemical reaction and are often due to the nature of the process. In processes such as drying, evaporation at the surface water body, energy transfer in a wet cooling tower and the flow in a desert cooler, heat and mass transfer occur simultaneously. In many of these processes, the interest lies in the determination of the total energy transfer, although in processes such as drying, the interest lies mainly on the overall mass transfer for moisture removal. Natural convection processes involving the combined mechanisms are also encountered in many natural processes, such as evaporation, condensation and agricultural drying, in many industrial applications involving solutions and mixtures in the absence of an externally induced flow and in many chemical processing systems. In many processes such as the curing of plastics, cleaning and chemical

processing of materials relevant to the manufacture of printed circuitry, manufacture of pulp-insulated cables etc., the combined buoyancy mechanisms arise and the total energy and material transfer resulting from the combined mechanisms, has to be determined.

The basic heat and mass transfer problem is governed by the combined buoyancy effects arising from the simultaneous diffusion of thermal energy and of chemical species. Therefore, the continuity, momentum, energy and concentration equations are coupled through the buoyancy terms alone, if the other effects, such as the Soret and Dufour effects are neglected. This would again be valid for low species concentration levels. These additional effects have also been considered in several investigations, for example, the work of Caldwell (1974), De Groot and Mazur (1962), and Hurle and Jakeman (1971).

### 1.3 Useful Dimensionless Parameters

#### Prandtl Number Pr

The Prandtl number is the ratio of kinematic viscosity to thermal diffusivity and may be written as follows,

$$\text{Pr} = \frac{\text{Kinematic viscosity}}{\text{Thermal diffusivity}} = \frac{\epsilon}{\frac{\lambda}{\rho c_p}} = \frac{\rho c_p \epsilon}{\lambda}$$

where  $c_p$  is the specific heat at constant pressure and  $\lambda$  is the thermal conductivity.

The value of  $\epsilon = \frac{\lambda}{\rho c_p}$  shows the effect of viscosity of the fluid. The smaller value of  $\epsilon$  is, the narrower is the region which is affected by viscosity and which is known as the boundary layer region when  $\epsilon$  is very small. The value of  $\frac{\lambda}{\rho c_p}$  shows the thermal diffusivity due to heat conduction. The smaller value of  $\frac{\lambda}{\rho c_p}$  is, the narrower is the region which is affected by the heat conduction and which is known as thermal boundary layer when  $\frac{\lambda}{\rho c_p}$  is small. Thus the Prandtl number shows that the relative importance of heat conduction and viscosity of a fluid.

Evidently, the value of Pr varies from fluid to fluid. For air at 20°C, Pr = 0.71 (approx.),

for water at 20°C, Pr = 7.0 (approx.), for mercury at 20°C, Pr = 0.044 (approx.) but for high viscous fluid it may be very large e.g. for glycerin at 20°C, Pr = 7250 (approx.).

### **Magnetic Parameter $M$**

This is obtained from the ratio of the magnetic force to the inertia force and is defined as,

$$M = \frac{\text{Magnetic force}}{\text{Inertia force}} = \frac{\sim_e B_0^2 \dagger L}{\dots U} = \frac{\sim_e^3 H_0^2 \dagger L}{\dots U},$$

where  $\sim_e$  is the magnetic permeability,  $\dagger$  is the electrical conductivity,  $H_0$  be the constant induced magnetic field.

### **Schmidt Number $Sc$**

It is the ratio of the viscous diffusivity to the chemical molecular diffusivity and is defined as,

$$Sc = \frac{\text{Visco sus diffusivity}}{\text{Chemical molecular diffusivity}} = \frac{\epsilon}{Dm}$$

### **Grashof Number $Gr$**

The Grashof number is defined as  $Gr = \frac{gS L^3 \nabla \bar{T}}{\epsilon^2}$ ,

where  $g$  is the local acceleration due to gravity,  $S$  is the thermal expansion coefficient and  $\nabla \bar{T}$  be the temperature difference.

It is a measure of the relative importance of buoyancy forces and viscous forces. The larger it is, stronger is the convective current.

### **Modified Grashof Number $Gm$**

This is defined as  $Gm = \frac{gS^* L^3 \nabla \bar{C}}{\epsilon^2}$

where  $S^*$  is the concentration expansion coefficient and  $\nabla \bar{C}$  be the concentration difference.

**Eckert Number  $Ec$** 

The Eckert number is defined as  $Ec = \frac{U^2}{c_p(\bar{T}_w - \bar{T}_\infty)}$ , which is the ratio of the kinetic energy at the wall to the specific enthalpy difference between wall and fluid. Eckert number phenomena is being the result of dissipation created by shear stress in the fluid at the wall. In other words, it is the kinetic energy of the flow relative to the enthalpy difference.

**Soret Number  $Sr$** 

The Soret Number is defined as  $Sr = \frac{D_m k_T (\bar{T}_w - \bar{T}_\infty)}{\epsilon T_m (\bar{C}_w - \bar{C}_\infty)}$

where  $k_T$  is the thermal diffusion ratio,  $T_m$  is the mean fluid temperature,  $\bar{T}_w$  and  $\bar{T}_\infty$  are temperature of the fluid at the wall and far away from the plate respectively as well as  $\bar{C}_w$  and  $\bar{C}_\infty$  are concentration of the species at the wall and far away from the plate respectively.

**Dufour Number,  $Du$** 

A dimensionless number used in studying thermo-diffusion, equal to the increase in enthalpy of a unit mass during isothermal mass transfer divided by the enthalpy of a unit mass of mixture.

The Dufour number is defined as  $Du = \frac{Dk_t (\bar{C}_w - \bar{C}_\infty)}{\dots c_s c_p (\bar{T}_w - \bar{T}_\infty)}$

## CHAPTER II

### Governing Equations

#### 2.1 Basic Governing Equations

From the basis of studying Magneto Fluid Dynamics, fluid flows for a combined heat and mass transfer are governed by the continuity equation, momentum equations, concentration equation, and energy equation together with the generalized Ohm's law and Maxwell's equations. The thermal-diffusion and diffusion-thermo effects together with viscous dissipation and Joule heating effect have been considered throughout the study.

The continuity equation for a viscous compressible electrically conducting fluid in vector form is

$$\frac{\partial \dots}{\partial t} + \nabla \cdot (\dots \mathbf{q}) = 0 \quad (2.1)$$

where  $\dots$  is the density of the fluid,  $\mathbf{q} = (u, v, w)$  is the fluid velocity vector in three dimensional Cartesian coordinate system. Here  $u$ ,  $v$  and  $w$  are the components of velocity vector in the  $x$ ,  $y$  and  $z$  directions respectively.

For incompressible fluid  $\dots = (\text{constant})$ , so that the equation (2.1) yields

$$\nabla \cdot \mathbf{q} = 0 \quad (2.2)$$

$$\text{i.e. } \frac{\partial u}{\partial x} + \frac{\partial v}{\partial y} + \frac{\partial w}{\partial z} = 0 \quad (2.3)$$

The Momentum equation for a viscous compressible fluid moves through a porous medium in vector form is

$$\frac{d\mathbf{q}}{dt} = \mathbf{F} - \frac{1}{\dots} \nabla P + \frac{\epsilon}{3} \nabla (\nabla \cdot \mathbf{q}) + \epsilon \nabla^2 \mathbf{q} - \frac{\sim}{\dots k_1} \mathbf{q} \quad (2.4)$$

where  $\mathbf{F} = (F_x, F_y, F_z)$  is the body force per unit mass;  $F_x$ ,  $F_y$ ,  $F_z$  be the components of the body force in the  $x$ ,  $y$ ,  $z$  directions respectively;  $P$  is the fluid pressure,  $\epsilon$  is the kinematic viscosity,  $\sim$  is the fluid viscosity and  $k_1$  is the permeability of the porous medium.

Since  $\frac{d\mathbf{q}}{dt} = \frac{\partial \mathbf{q}}{\partial t} + (\mathbf{q} \cdot \nabla) \mathbf{q}$  and for incompressible fluid  $\nabla \cdot \mathbf{q} = 0$  so the equation (2.4)

becomes

$$\frac{\partial \mathbf{q}}{\partial t} + (\mathbf{q} \cdot \nabla) \mathbf{q} = \mathbf{F} - \frac{1}{\dots} \nabla P + \epsilon \nabla^2 \mathbf{q} - \frac{\sim}{\dots k_1} \mathbf{q} \quad (2.5)$$

A strong uniform magnetic field  $\mathbf{B} = (0, B_0, 0)$  is imposed along the y-axis and the magnetic Reynolds number of the flow is assumed to be small enough so that the included magnetic field is negligible in comparison with applied magnetic field. The magnetic lines are fixed relative to the fluid. Using the relation  $\nabla \cdot \mathbf{J} = 0$  for the current density  $\mathbf{J} = (J_x, J_y, J_z)$  where  $J_y = \text{constant}$ . Since the plate is non-conducting,  $J_y = 0$  at the plate and hence zero everywhere. The generalized Ohm's law in the absence of electric field to the case of short circuit problem (Meyer (1958) and Cowling (1956));

$$\mathbf{J} = \dagger \left( \mathbf{q} \wedge \mathbf{B} + \frac{1}{ne} \text{grad } p_e \right) - \frac{S_e}{B_0} (\mathbf{J} \wedge \mathbf{B}) + \frac{S_i S_e}{B_0} (\mathbf{J} \wedge \mathbf{B}) \wedge \mathbf{B}$$

where  $\dagger$ ,  $\sim$ ,  $n$ ,  $e$ ,  $p_e$ ,  $S_e$  and  $S_i$  are the electric conductivity, the magnetic permeability, the number density of electron, the electric charge, the electron pressure, Hall parameter, and Ion-slip parameter, respectively. If we neglect the electron pressure, Hall parameter, and Ion-slip parameter, we have

$$J_x = -\dagger B_0 w$$

$$J_z = \dagger B_0 u$$

Then the equation (2.5) becomes as following form

$$\frac{\partial \mathbf{q}}{\partial t} + (\mathbf{q} \cdot \nabla) \mathbf{q} = \mathbf{F} - \frac{1}{\dots} \nabla P + \epsilon \nabla^2 \mathbf{q} + \frac{1}{\dots} (\mathbf{J} \wedge \mathbf{B}) - \frac{\sim}{\dots k_1} \mathbf{q} \quad (2.6)$$

$$\text{Now } \mathbf{q} \cdot \nabla = (u, v, w) \cdot \left( \frac{\partial}{\partial x}, \frac{\partial}{\partial y}, \frac{\partial}{\partial z} \right) = u \frac{\partial}{\partial x} + v \frac{\partial}{\partial y} + w \frac{\partial}{\partial z} \quad (2.7)$$

$$\begin{aligned} \therefore (\mathbf{q} \cdot \nabla) \mathbf{q} &= \left( u \frac{\partial}{\partial x} + v \frac{\partial}{\partial y} + w \frac{\partial}{\partial z} \right) (u, v, w) \\ &= \left( \left( u \frac{\partial u}{\partial x} + v \frac{\partial u}{\partial y} + w \frac{\partial u}{\partial z} \right), \left( u \frac{\partial v}{\partial x} + v \frac{\partial v}{\partial y} + w \frac{\partial v}{\partial z} \right), \left( u \frac{\partial w}{\partial x} + v \frac{\partial w}{\partial y} + w \frac{\partial w}{\partial z} \right) \right) \end{aligned} \quad (2.8)$$

$$\nabla P = \left( \frac{\partial P}{\partial x}, \frac{\partial P}{\partial y}, \frac{\partial P}{\partial z} \right) \quad (2.9)$$

$$\nabla^2 \mathbf{q} = \left( \frac{\partial^2}{\partial x^2} + \frac{\partial^2}{\partial y^2} + \frac{\partial^2}{\partial z^2} \right) (u, v, w)$$



$$= \left( \left( \frac{\partial^2 u}{\partial x^2} + \frac{\partial^2 u}{\partial y^2} + \frac{\partial^2 u}{\partial z^2} \right), \left( \frac{\partial^2 v}{\partial x^2} + \frac{\partial^2 v}{\partial y^2} + \frac{\partial^2 v}{\partial z^2} \right), \left( \frac{\partial^2 w}{\partial x^2} + \frac{\partial^2 w}{\partial y^2} + \frac{\partial^2 w}{\partial z^2} \right) \right) \quad (2.10)$$

$$\mathbf{J} = (-\dagger B_0 w, 0, \dagger B_0 u) \quad (2.11)$$

$$\text{and } \mathbf{J} \wedge \mathbf{B} = (-\dagger B_0^2 u, 0, \dagger B_0^2 w) \quad (2.12)$$

In three-dimensional Cartesian coordinate system the momentum equation (2.6) with the help of the equations (2.7)-(2.12) become,

$$\frac{\partial u}{\partial t} + u \frac{\partial u}{\partial x} + v \frac{\partial u}{\partial y} + w \frac{\partial u}{\partial z} = F_x - \frac{1}{\dots} \frac{\partial P}{\partial x} + \epsilon \left( \frac{\partial^2 u}{\partial x^2} + \frac{\partial^2 u}{\partial y^2} + \frac{\partial^2 u}{\partial z^2} \right) - \frac{\dagger B_0^2 u}{\dots} - \frac{\sim}{\dots k_1} u \quad (2.13)$$

$$\frac{\partial v}{\partial t} + u \frac{\partial v}{\partial x} + v \frac{\partial v}{\partial y} + w \frac{\partial v}{\partial z} = F_y - \frac{1}{\dots} \frac{\partial P}{\partial y} + \epsilon \left( \frac{\partial^2 v}{\partial x^2} + \frac{\partial^2 v}{\partial y^2} + \frac{\partial^2 v}{\partial z^2} \right) - \frac{\sim}{\dots k_1} v \quad (2.14)$$

$$\frac{\partial w}{\partial t} + u \frac{\partial w}{\partial x} + v \frac{\partial w}{\partial y} + w \frac{\partial w}{\partial z} = F_z - \frac{1}{\dots} \frac{\partial P}{\partial z} + \epsilon \left( \frac{\partial^2 w}{\partial x^2} + \frac{\partial^2 w}{\partial y^2} + \frac{\partial^2 w}{\partial z^2} \right) + \frac{\dagger B_0^2 w}{\dots} - \frac{\sim}{\dots k_1} w \quad (2.15)$$

The concentration equation for a viscous incompressible electrically conducting fluid with thermal-diffusion is;

$$\frac{\partial \bar{C}}{\partial t} + (\mathbf{q} \cdot \nabla) \bar{C} = D \nabla^2 \bar{C} + \frac{Dk_t}{T_m} \nabla^2 \bar{T} \quad (2.16)$$

where  $C$  is the concentration variable of the species,  $\bar{T}$  is the fluid temperature,  $D$  is the coefficient of mass diffusivity,  $k_t$  is the thermal diffusion ratio and  $T_m$  is the mean fluid temperature. Also using the equation (2.1.3) we have

$$(\mathbf{q} \cdot \nabla) \bar{C} = u \frac{\partial \bar{C}}{\partial x} + v \frac{\partial \bar{C}}{\partial y} + w \frac{\partial \bar{C}}{\partial z} \quad (2.17)$$

$$\nabla^2 \bar{C} = \frac{\partial^2 \bar{C}}{\partial x^2} + \frac{\partial^2 \bar{C}}{\partial y^2} + \frac{\partial^2 \bar{C}}{\partial z^2} \quad (2.18)$$

$$\nabla^2 \bar{T} = \frac{\partial^2 \bar{T}}{\partial x^2} + \frac{\partial^2 \bar{T}}{\partial y^2} + \frac{\partial^2 \bar{T}}{\partial z^2} \quad (2.19)$$

In three-dimensional Cartesian coordinate system the concentration equation (2.16) with the help of the equations (2.17)-(2.19) become

$$\frac{\partial \bar{C}}{\partial t} + u \frac{\partial \bar{C}}{\partial x} + v \frac{\partial \bar{C}}{\partial y} + w \frac{\partial \bar{C}}{\partial z} = D \left( \frac{\partial^2 \bar{C}}{\partial x^2} + \frac{\partial^2 \bar{C}}{\partial y^2} + \frac{\partial^2 \bar{C}}{\partial z^2} \right) + \frac{Dk_t}{T_m} \left( \frac{\partial^2 \bar{T}}{\partial x^2} + \frac{\partial^2 \bar{T}}{\partial y^2} + \frac{\partial^2 \bar{T}}{\partial z^2} \right) \quad (2.20)$$

The energy equation for a viscous incompressible electrically conducting fluid with diffusion-thermo effect, Joule heating and viscous dissipation term is

$$\frac{\partial \bar{T}}{\partial t} + (\mathbf{q} \cdot \nabla) \bar{T} = \frac{1}{\dots c_p} \nabla \cdot (K(\bar{T}) \nabla \bar{T}) + \frac{Dk_t}{c_s c_p} \nabla^2 \bar{C} + \frac{\mathbf{J}^2}{\dots c_p \dagger_1} + \frac{1}{\dots c_p} \{ \quad \quad \quad \} \quad (2.21)$$

Where  $c_p$  is the specific heat at the constant pressure,  $c_s$  is the concentration susceptibility and  $K(\bar{T}) = K_0 [1 + \alpha_1 (\bar{T} - \bar{T}_\infty)]$ ,  $K_0$  is the thermal conductivity of the ambient fluid.

$$\{ = \sim \left[ 2 \left\{ \left( \frac{\partial u}{\partial x} \right)^2 + \left( \frac{\partial v}{\partial y} \right)^2 + \left( \frac{\partial w}{\partial z} \right)^2 \right\} + \left( \frac{\partial v}{\partial x} + \frac{\partial u}{\partial y} \right)^2 + \left( \frac{\partial w}{\partial y} + \frac{\partial v}{\partial z} \right)^2 + \left( \frac{\partial u}{\partial z} + \frac{\partial w}{\partial x} \right)^2 \right].$$

Also  $\{$  denotes the dissipation function involving the viscous stress and it represents the rate at which energy is being dissipated per unit volume through the action of viscosity. In fact the energy is dissipated in a viscous fluid in motion on account of internal friction given for incompressible fluid. This is always positive, since all the terms are quadratic.

Again using the equation (2.7) we have

$$(\mathbf{q} \cdot \nabla) \bar{T} = u \frac{\partial \bar{T}}{\partial x} + v \frac{\partial \bar{T}}{\partial y} + w \frac{\partial \bar{T}}{\partial z} \quad (2.22)$$

$$\nabla \bar{T} = \left( \frac{\partial \bar{T}}{\partial x}, \frac{\partial \bar{T}}{\partial y}, \frac{\partial \bar{T}}{\partial z} \right) \quad (2.23)$$

and from the equation (2.11) we have

$$\mathbf{J}^2 = \dagger^2 B_0^2 (u^2 + w^2) \quad (2.24)$$

In three-dimensional Cartesian coordinate system the energy equation (2.21) with the help of the equations (2.22) – (2.24) become

$$\begin{aligned} \frac{\partial \bar{T}}{\partial t} + u \frac{\partial \bar{T}}{\partial x} + v \frac{\partial \bar{T}}{\partial y} + w \frac{\partial \bar{T}}{\partial z} = \frac{1}{\dots c_p} \left[ \frac{\partial}{\partial x} \left( K(\bar{T}) \frac{\partial \bar{T}}{\partial x} \right) + \frac{\partial}{\partial y} \left( K(\bar{T}) \frac{\partial \bar{T}}{\partial y} \right) + \frac{\partial}{\partial z} \left( K(\bar{T}) \frac{\partial \bar{T}}{\partial z} \right) \right] \\ + \frac{Dk_t}{c_s c_p} \left( \frac{\partial^2 \bar{C}}{\partial x^2} + \frac{\partial^2 \bar{C}}{\partial y^2} + \frac{\partial^2 \bar{C}}{\partial z^2} \right) + \frac{\dagger_1 B_0^2 (u^2 + w^2)}{\dots c_p} \\ + \frac{\epsilon}{c_p} \left[ 2 \left\{ \left( \frac{\partial u}{\partial x} \right)^2 + \left( \frac{\partial v}{\partial y} \right)^2 + \left( \frac{\partial w}{\partial z} \right)^2 \right\} + \left( \frac{\partial v}{\partial x} + \frac{\partial u}{\partial y} \right)^2 + \left( \frac{\partial w}{\partial y} + \frac{\partial v}{\partial z} \right)^2 + \left( \frac{\partial u}{\partial z} + \frac{\partial w}{\partial x} \right)^2 \right] \quad (2.25) \end{aligned}$$

In three-dimensional Cartesian coordinate system the continuity equation (2.3), the momentum equations (2.13) – (2.15), the concentration equation (2.20) and the energy equation (2.25) are as follows

**The Continuity equation:**

$$\frac{\partial u}{\partial x} + \frac{\partial v}{\partial y} + \frac{\partial w}{\partial z} = 0$$

**The Momentum equations:**

$$\frac{\partial u}{\partial t} + u \frac{\partial u}{\partial x} + v \frac{\partial u}{\partial y} + w \frac{\partial u}{\partial z} = F_x - \frac{1}{\dots} \frac{\partial P}{\partial x} + \epsilon \left( \frac{\partial^2 u}{\partial x^2} + \frac{\partial^2 u}{\partial y^2} + \frac{\partial^2 u}{\partial z^2} \right) - \frac{\dagger B_0^2 u}{\dots} - \frac{\sim}{\dots k_1} u$$

$$\frac{\partial v}{\partial t} + u \frac{\partial v}{\partial x} + v \frac{\partial v}{\partial y} + w \frac{\partial v}{\partial z} = F_y - \frac{1}{\dots} \frac{\partial P}{\partial y} + \epsilon \left( \frac{\partial^2 v}{\partial x^2} + \frac{\partial^2 v}{\partial y^2} + \frac{\partial^2 v}{\partial z^2} \right) - \frac{\sim}{\dots k_1} v$$

$$\frac{\partial w}{\partial t} + u \frac{\partial w}{\partial x} + v \frac{\partial w}{\partial y} + w \frac{\partial w}{\partial z} = F_z - \frac{1}{\dots} \frac{\partial P}{\partial z} + \epsilon \left( \frac{\partial^2 w}{\partial x^2} + \frac{\partial^2 w}{\partial y^2} + \frac{\partial^2 w}{\partial z^2} \right) + \frac{\dagger B_0^2 w}{\dots} - \frac{\sim}{\dots k_1} w$$

**The Concentration equation:**

$$\frac{\partial \bar{C}}{\partial t} + u \frac{\partial \bar{C}}{\partial x} + v \frac{\partial \bar{C}}{\partial y} + w \frac{\partial \bar{C}}{\partial z} = D \left( \frac{\partial^2 \bar{C}}{\partial x^2} + \frac{\partial^2 \bar{C}}{\partial y^2} + \frac{\partial^2 \bar{C}}{\partial z^2} \right) + \frac{Dk_t}{T_m} \left( \frac{\partial^2 \bar{T}}{\partial x^2} + \frac{\partial^2 \bar{T}}{\partial y^2} + \frac{\partial^2 \bar{T}}{\partial z^2} \right)$$

**The Energy equation:**

$$\begin{aligned} \frac{\partial \bar{T}}{\partial t} + u \frac{\partial \bar{T}}{\partial x} + v \frac{\partial \bar{T}}{\partial y} + w \frac{\partial \bar{T}}{\partial z} &= \frac{1}{\dots c_p} \left[ \frac{\partial}{\partial x} \left( K(\bar{T}) \frac{\partial \bar{T}}{\partial x} \right) + \frac{\partial}{\partial y} \left( K(\bar{T}) \frac{\partial \bar{T}}{\partial y} \right) + \frac{\partial}{\partial z} \left( K(\bar{T}) \frac{\partial \bar{T}}{\partial z} \right) \right] \\ &+ \frac{Dk_t}{c_s c_p} \left( \frac{\partial^2 \bar{C}}{\partial x^2} + \frac{\partial^2 \bar{C}}{\partial y^2} + \frac{\partial^2 \bar{C}}{\partial z^2} \right) + \frac{\dagger_1 B_0^2 (u^2 + w^2)}{\dots c_p} \\ &+ \frac{\epsilon}{c_p} \left[ 2 \left\{ \left( \frac{\partial u}{\partial x} \right)^2 + \left( \frac{\partial v}{\partial y} \right)^2 + \left( \frac{\partial w}{\partial z} \right)^2 \right\} + \left( \frac{\partial v}{\partial x} + \frac{\partial u}{\partial y} \right)^2 + \left( \frac{\partial w}{\partial y} + \frac{\partial v}{\partial z} \right)^2 + \left( \frac{\partial u}{\partial z} + \frac{\partial w}{\partial x} \right)^2 \right] \end{aligned}$$

Consider an unsteady fluid flow for a combined heat and mass transfer past an electrically non-conducting continuously moving semi-infinite impulsive vertical porous plate. It has been considered the effect of thermal-diffusion, diffusion-thermo, Joule heating effect and viscous dissipation effect. The physical configuration and coordinate system are shown in Figure 2.1

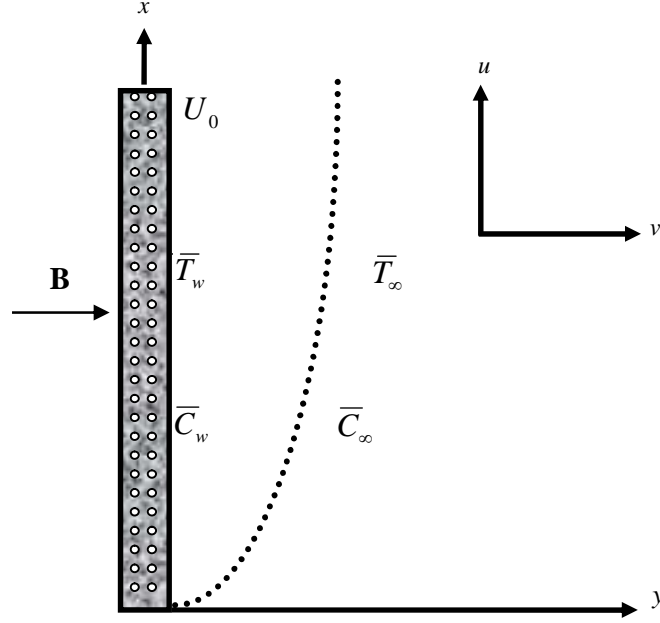


**Figure 2.1:** Physical configuration and coordinate system.

The flow is assumed to be in the  $x$ -direction which is taken along the plate in upward direction and  $y$ -axis is normal to it. The leading edge of the plate is taken as coincident with  $z$ -axis. Hence mathematically we can write  $\frac{\partial}{\partial z} \equiv 0$ . A uniform magnetic field  $B_0$  can be taken as  $(0, B_0, 0)$  to the considered plate which is assumed to be electrically non-conducting.

$$\frac{\partial u}{\partial x} + \frac{\partial v}{\partial y} = 0 \quad (2.26)$$

$$\frac{\partial u}{\partial t} + u \frac{\partial u}{\partial x} + v \frac{\partial u}{\partial y} = F_x - \frac{1}{\dots} \frac{\partial P}{\partial x} + \epsilon \left( \frac{\partial^2 u}{\partial x^2} + \frac{\partial^2 u}{\partial y^2} \right) - \frac{\dagger B_0^2 u}{\dots} - \frac{\sim}{\dots k_1} u \quad (2.27)$$

$$\frac{\partial v}{\partial t} + u \frac{\partial v}{\partial x} + v \frac{\partial v}{\partial y} = F_y - \frac{1}{\dots} \frac{\partial P}{\partial y} + \epsilon \left( \frac{\partial^2 v}{\partial x^2} + \frac{\partial^2 v}{\partial y^2} \right) - \frac{\sim}{\dots k_1} v \quad (2.28)$$

$$\frac{\partial w}{\partial t} + u \frac{\partial w}{\partial x} + v \frac{\partial w}{\partial y} = F_z - \frac{1}{\dots} \frac{\partial P}{\partial z} + \epsilon \left( \frac{\partial^2 w}{\partial x^2} + \frac{\partial^2 w}{\partial y^2} \right) + \frac{\dagger B_0^2 w}{\dots} - \frac{\sim}{\dots k_1} w \quad (2.29)$$

$$\frac{\partial \bar{C}}{\partial t} + u \frac{\partial \bar{C}}{\partial x} + v \frac{\partial \bar{C}}{\partial y} = D \left( \frac{\partial^2 \bar{C}}{\partial x^2} + \frac{\partial^2 \bar{C}}{\partial y^2} \right) + \frac{Dk_t}{T_m} \left( \frac{\partial^2 \bar{T}}{\partial x^2} + \frac{\partial^2 \bar{T}}{\partial y^2} \right) \quad (2.30)$$

$$\begin{aligned}
\frac{\partial \bar{T}}{\partial t} + u \frac{\partial \bar{T}}{\partial x} + v \frac{\partial \bar{T}}{\partial y} &= \frac{1}{\dots c_p} \left[ \frac{\partial}{\partial x} \left( K(\bar{T}) \frac{\partial \bar{T}}{\partial x} \right) + \frac{\partial}{\partial y} \left( K(\bar{T}) \frac{\partial \bar{T}}{\partial y} \right) \right] + \frac{Dk_t}{c_s c_p} \left( \frac{\partial^2 \bar{C}}{\partial x^2} + \frac{\partial^2 \bar{C}}{\partial y^2} \right) \\
+ \frac{\dagger_1 B_0^2 (u^2 + w^2)}{\dots c_p} + \frac{\epsilon}{c_p} &\left[ 2 \left\{ \left( \frac{\partial u}{\partial x} \right)^2 + \left( \frac{\partial v}{\partial y} \right)^2 \right\} + \left( \frac{\partial v}{\partial x} + \frac{\partial u}{\partial y} \right)^2 + \left( \frac{\partial w}{\partial y} \right)^2 + \left( \frac{\partial w}{\partial x} \right)^2 \right] \quad (2.31)
\end{aligned}$$

Initially the plate as well as the fluid is at the same temperature  $\bar{T}(=\bar{T}_\infty)$  and the concentration level  $\bar{C}(=\bar{C}_\infty)$  everywhere in the fluid is same. Also the fluid and the plate is at rest. After that the plate is to be moving with a constant velocity  $U_0$  in its own plane and instantaneously at time  $t > 0$ , the temperature of the plate and the concentration are raised to  $\bar{T}_w (> \bar{T}_\infty)$  and  $\bar{C}_w (\geq \bar{C}_\infty)$  respectively, which are thereafter maintained constant, where  $\bar{T}_w$ ,  $\bar{C}_w$  are the temperature and concentration at the wall and  $\bar{T}_\infty$ ,  $\bar{C}_\infty$  are the temperature and concentration far away from the plate respectively.

The  $x$ -component of momentum equation (2.13) reduces if the only contribution to the body force is made by gravity, the body force per unit volume,  $F_x = -g$ , where  $g$  is the local acceleration due to gravity. There is no body force in the  $y$  and  $z$ -directions, that is,  $F_y = F_z = 0$ . Thus  $\frac{\partial P}{\partial y} = 0$  which implies that  $P = P(x)$ . Hence the  $x$ -component of pressure gradient at any point in the boundary layer must equal to the pressure gradient in the quiescent region outside the boundary layer. However, in this region  $u = v = w$ . Therefore the  $x$ -component of pressure gradient of the momentum equation,  $\frac{\partial P}{\partial x} = -\dots_\infty g$ , where  $\dots_\infty$  is the density of the surrounding fluid at the temperature  $\bar{T}_\infty$ .

$$\begin{aligned}
\text{Therefore, } F_x - \frac{1}{\dots} \frac{\partial P}{\partial x} &= -g + \frac{g \dots_\infty}{\dots} \\
&= -g \left( \frac{\dots - \dots_\infty}{\dots} \right).
\end{aligned}$$

For small differences, the density difference term  $\dots - \dots_\infty$  is related to the temperature difference  $\bar{T} - \bar{T}_\infty$  and the mass difference  $\bar{C} - \bar{C}_\infty$  through the thermal expansion coefficient  $S_T$  and the concentration expansion coefficient  $S_C$  by the relation

$$\frac{\dots - \dots_\infty}{\dots} = -S_T (\bar{T} - \bar{T}_\infty) - S_C (\bar{C} - \bar{C}_\infty)$$

$$\therefore F_x - \frac{1}{\dots} \frac{\partial P}{\partial x} = gS_T(\bar{T} - \bar{T}_\infty) + gS_C(\bar{C} - \bar{C}_\infty) \quad (2.32)$$

Hence the continuity equation (2.26), the momentum equations (2.27) – (2.29), the concentration equation (2.30) and the energy equation (2.31) become

$$\frac{\partial u}{\partial x} + \frac{\partial v}{\partial y} = 0 \quad (2.33)$$

$$\frac{\partial u}{\partial t} + u \frac{\partial u}{\partial x} + v \frac{\partial u}{\partial y} = \epsilon \left( \frac{\partial^2 u}{\partial x^2} + \frac{\partial^2 u}{\partial y^2} \right) + gS_T(\bar{T} - \bar{T}_\infty) + gS_C(\bar{C} - \bar{C}_\infty) - \frac{\dagger B_0^2 u}{\dots} - \frac{\sim}{\dots k_1} u \quad (2.34)$$

$$\frac{\partial v}{\partial t} + u \frac{\partial v}{\partial x} + v \frac{\partial v}{\partial y} = \epsilon \left( \frac{\partial^2 v}{\partial x^2} + \frac{\partial^2 v}{\partial y^2} \right) - \frac{\sim}{\dots k_1} v \quad (2.35)$$

$$\frac{\partial w}{\partial t} + u \frac{\partial w}{\partial x} + v \frac{\partial w}{\partial y} = \epsilon \left( \frac{\partial^2 w}{\partial x^2} + \frac{\partial^2 w}{\partial y^2} \right) + \frac{\dagger B_0^2 w}{\dots} - \frac{\sim}{\dots k_1} w \quad (2.36)$$

$$\frac{\partial \bar{C}}{\partial t} + u \frac{\partial \bar{C}}{\partial x} + v \frac{\partial \bar{C}}{\partial y} = D \left( \frac{\partial^2 \bar{C}}{\partial x^2} + \frac{\partial^2 \bar{C}}{\partial y^2} \right) + \frac{Dk_t}{T_m} \left( \frac{\partial^2 \bar{T}}{\partial x^2} + \frac{\partial^2 \bar{T}}{\partial y^2} \right) \quad (2.37)$$

$$\begin{aligned} \frac{\partial \bar{T}}{\partial t} + u \frac{\partial \bar{T}}{\partial x} + v \frac{\partial \bar{T}}{\partial y} = & \frac{1}{\dots c_p} \left[ \frac{\partial}{\partial x} \left( K(\bar{T}) \frac{\partial \bar{T}}{\partial x} \right) + \frac{\partial}{\partial y} \left( K(\bar{T}) \frac{\partial \bar{T}}{\partial y} \right) \right] + \frac{Dk_t}{c_s c_p} \left( \frac{\partial^2 \bar{C}}{\partial x^2} + \frac{\partial^2 \bar{C}}{\partial y^2} \right) \\ & + \frac{\dagger_1 B_0^2 (u^2 + w^2)}{\dots c_p} + \frac{\epsilon}{c_p} \left[ 2 \left\{ \left( \frac{\partial u}{\partial x} \right)^2 + \left( \frac{\partial v}{\partial y} \right)^2 \right\} + \left( \frac{\partial v}{\partial x} + \frac{\partial u}{\partial y} \right)^2 + \left( \frac{\partial w}{\partial y} \right)^2 + \left( \frac{\partial w}{\partial x} \right)^2 \right] \end{aligned} \quad (2.38)$$

If the plate is infinite in extent then all physical quantities depend on  $y$  and  $t$ . Thus under the Boussinesq approximations and by neglecting the small order terms, the continuity equation (2.33), the momentum equations (2.34) – (2.36), the concentration equation (2.37) and the energy equation (2.38) become

$$\frac{\partial v}{\partial y} = 0 \quad (2.39)$$

$$\frac{\partial u}{\partial t} - v_0 \frac{\partial u}{\partial y} = \epsilon \frac{\partial^2 u}{\partial y^2} + gS_T(\bar{T} - \bar{T}_\infty) + gS_C(\bar{C} - \bar{C}_\infty) - \frac{\dagger B_0^2 u}{\dots} - \frac{\sim}{\dots k_1} u \quad (2.40)$$

$$\frac{\partial \bar{C}}{\partial t} - v_0 \frac{\partial \bar{C}}{\partial y} = D \frac{\partial^2 \bar{C}}{\partial y^2} + \frac{Dk_t}{T_m} \frac{\partial^2 \bar{T}}{\partial y^2} \quad (2.41)$$

$$\frac{\partial \bar{T}}{\partial t} - v_0 \frac{\partial \bar{T}}{\partial y} = \frac{1}{\dots c_p} \frac{\partial}{\partial y} \left( K(\bar{T}) \frac{\partial \bar{T}}{\partial y} \right) + \frac{Dk_t}{c_s c_p} \frac{\partial^2 \bar{C}}{\partial y^2} + \frac{\dagger_1 B_0^2 u^2}{\dots c_p} + \frac{\epsilon}{c_p} \left( \frac{\partial u}{\partial y} \right)^2 \quad (2.42)$$

where  $K(\bar{T}) = K_0 [1 + \chi_1 (\bar{T} - \bar{T}_\infty)]$  and  $v_0$  is the suction velocity.

The corresponding initial and boundary conditions are prescribed as follows:

$$t \leq 0, u = 0, \bar{T} \rightarrow \bar{T}_\infty, \bar{C} \rightarrow \bar{C}_\infty \text{ for all } y \quad (2.43)$$

$$t > 0, u = U_0, \bar{T} \rightarrow \bar{T}_w, \bar{C} \rightarrow \bar{C}_w \text{ at } y = 0$$

$$u \rightarrow 0, \bar{T} \rightarrow \bar{T}_\infty, \bar{C} \rightarrow \bar{C}_\infty \text{ as } y \rightarrow \infty \quad (4.44)$$

## CHAPTER V

### Conclusions

The finite difference solution of MHD mixed convection flow through an impulsively started permeable vertical plate with diffusion-thermo and thermal-diffusion effects have been investigated.

Some important findings of this investigation are listed below;

1. The fluid velocity increases with the increase of Grashof Number, Modified Grashof Number, Dufour Number, Soret Number, Eckert Number, and Variable thermal conductivity Parameter.
2. Reverse effects are observed with the increase of Prandtl Number, Schmidt Number, Magnetic Parameter, Permeability of the porous medium and Suction Parameter.
3. The fluid temperature increases with the increase of Grashof Number, Modified Grashof Number, Dufour Number, Soret Number, Eckert Number, and Variable thermal conductivity parameter.
4. Reverse effects are seen with the increase of Prandtl Number, Magnetic Parameter, Permeability of the porous medium and Suction Parameter.
5. The fluid concentration increases with the increase of Soret Number and reverse effect are observed with the increase of Schmidt Number and Suction Parameter.
6. There is no significant effect of the observed parameters on the concentration distributions except Schmidt number, Soret number and suction parameter. Here concentration profiles are decreasing with the increase of both  $Sc$  and  $\lambda$ , but it decreased quickly with the increase of the suction parameter  $\lambda$ . It On the other hand concentration profiles show increasing behaviour with the increase of Soret number,  $Sr$ .



As the basis for many engineering and scientific applications, for study more complex problems involving the MHD flow, it is hoped that the findings of this investigation may be useful for study of movement oil or gas and water through the reservoir of an oil or gas field, in the migration of underground water or oil as well as in the filtration and water purification processes. These results may also be useful for plasma studies as well as in power engineering, geothermal energy extractions, geophysics and astrophysics.

## CHAPTER III

### Calculation Technique

Many physical phenomena in applied science and engineering when formulated into mathematical models fall into a category of systems known as non-linear coupled partial differential equations. Most of these problems can be formulated as second order partial differential equations. A system of non-linear coupled partial differential equations with the boundary conditions are very difficult to solve analytically. For obtaining the solution of such problems advanced numerical methods have been employed. The governing equations of our problem contain a system of partial differential equations which are transformed by usual transformation into a non-dimensional system of non-linear coupled partial differential equations with boundary conditions. Hence the solution of our problem would be accomplished by the advanced numerical method, the Finite Difference numerical method has been used for solving our obtained non-similar coupled partial differential equations.

#### 3.1. Finite Difference Method

In order to solve the governing partial differential equations by Finite Difference Method, let us consider a two-dimensional region as shown in Figure 3.1. It is covered by a rectangular grid formed by two sets of lines drawn parallel to the coordinate axes with grid spacing  $\Delta x$  and  $\Delta y$  in  $x$  and  $y$  directions respectively.

The numerical values of the dependent variables are obtained at the points of intersection of the parallel lines, called *mesh* points, *lattice* points or *nodal* points. These values are obtained by discretizing the governing partial differential equations over the region of interest to derive approximately equivalent algebraic equations. The discretization consists

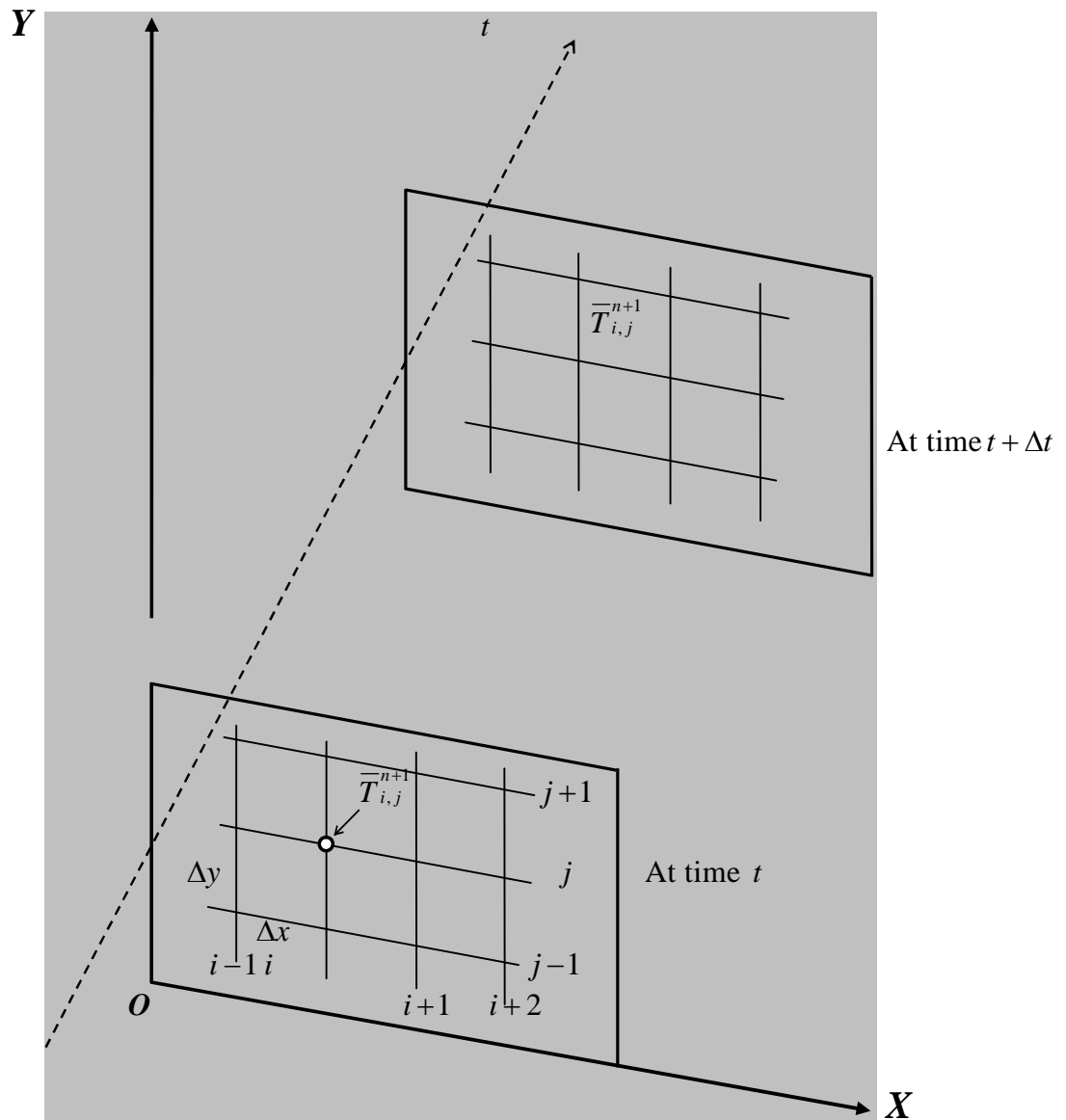


**Figure 3.1:** Space-Time index notation

of replacing each derivative of the partial differential equation at a mesh point by a finite difference approximation in terms of the values of the dependent variable at the mesh point and at the immediate neighboring mesh points and boundary points. In doing so, a set of algebraic equations arise.

Let the temperature  $\bar{T}$  at a representative point be a function of two special coordinates  $x$ ,  $y$  and time  $t$ . We adopt the following notation:

Let the subscripts  $i$  and  $j$  represent  $x$  and  $y$  coordinates and superscript  $n$  represents time. Let the mesh spacing in  $x$  and  $y$  directions are denoted by  $\Delta x$  and  $\Delta y$  also the time step by  $\Delta t$ . Thus  $\bar{T}(x, y, t)$  can be represented by  $\bar{T}(i\Delta x, j\Delta y, n\Delta t) = \bar{T}_{i,j}^n$ . With this notation, let us assume that the function  $\bar{T}$  and its derivatives are continuous. Then from Taylor's series expansions, the finite difference approximations to derivatives can be obtained. For example, the Taylor's series expansion of  $\bar{T}_{i+1,j}$  about the grid point  $(i, j)$  gives

$$\bar{T}_{i+1,j} = \bar{T}_{i,j} + \left[ \Delta x \frac{\partial \bar{T}}{\partial x} + \frac{(\Delta x)^2}{2!} \frac{\partial^2 \bar{T}}{\partial x^2} + \frac{(\Delta x)^3}{3!} \frac{\partial^3 \bar{T}}{\partial x^3} + \frac{(\Delta x)^4}{4!} \frac{\partial^4 \bar{T}}{\partial x^4} + \text{higher order terms} \right]_{i,j} \quad (3.1)$$

or,  $\left( \frac{\partial \bar{T}}{\partial x} \right)_{i,j} = \frac{\bar{T}_{i+1,j} - \bar{T}_{i,j}}{\Delta x} + O(\Delta x)$  which is the forward difference approximation to the

derivative  $\frac{\partial \bar{T}}{\partial x}$  with a truncation error of order  $\Delta x$ .

Similarly,

$$\bar{T}_{i-1,j} = \bar{T}_{i,j} - \left[ \Delta x \frac{\partial \bar{T}}{\partial x} - \frac{(\Delta x)^2}{2!} \frac{\partial^2 \bar{T}}{\partial x^2} + \frac{(\Delta x)^3}{3!} \frac{\partial^3 \bar{T}}{\partial x^3} - \frac{(\Delta x)^4}{4!} \frac{\partial^4 \bar{T}}{\partial x^4} + \text{higher order terms} \right]_{i,j} \quad (3.2)$$

or,  $\left( \frac{\partial \bar{T}}{\partial x} \right)_{i,j} = \frac{\bar{T}_{i,j} - \bar{T}_{i-1,j}}{\Delta x} + O(\Delta x)$  which is the backward difference approximation to the

derivative  $\frac{\partial \bar{T}}{\partial x}$  with a truncation error of order  $\Delta x$ .

Both approximations are first order accurate.

Subtracting equation (3.2) from equation (3.1), we obtain

$$\left( \frac{\partial \bar{T}}{\partial x} \right)_{i,j} = \frac{\bar{T}_{i+1,j} - \bar{T}_{i-1,j}}{2\Delta x} + [O(\Delta x)^2].$$

This is a central difference approximation to the derivative  $\frac{\partial \bar{T}}{\partial x}$  with a truncation error of order  $(\Delta x)^2$ , which is second order accurate.

The central difference approximation to a second order partial derivative  $\frac{\partial^2 \bar{T}}{\partial x^2}$  can be similarly obtained by adding the equations (3.1) and (3.2).

$$\text{Thus } \left( \frac{\partial^2 \bar{T}}{\partial x^2} \right)_{i,j} = \frac{\bar{T}_{i+1,j} - 2\bar{T}_{i,j} + \bar{T}_{i-1,j}}{\Delta x^2} + [O(\Delta x)^2]$$

Similar expressions can be written for  $y$  derivatives.

$$\left( \frac{\partial^2 \bar{T}}{\partial y^2} \right)_{i,j} = \frac{\bar{T}_{i,j+1} - 2\bar{T}_{i,j} + \bar{T}_{i,j-1}}{\Delta y^2} + [O(\Delta y)^2]$$

which are also second order accurate.

The expressions for mixed derivatives can be obtained by differentiating with respect to each variable in turn. Thus for example,

$$\left( \frac{\partial^2 \bar{T}}{\partial x \partial y} \right)_{i,j} = \frac{\partial}{\partial x} \left( \frac{\partial \bar{T}}{\partial y} \right)_{i,j} = \frac{\left( \frac{\partial \bar{T}}{\partial y} \right)_{i+1,j} - \left( \frac{\partial \bar{T}}{\partial y} \right)_{i-1,j}}{2\Delta x} = \frac{\left( \frac{\bar{T}_{i+1,j+1} - \bar{T}_{i+1,j-1}}{2\Delta y} \right) - \left( \frac{\bar{T}_{i-1,j+1} - \bar{T}_{i-1,j-1}}{2\Delta y} \right)}{2\Delta x}$$

Therefore,

$$\left( \frac{\partial^2 \bar{T}}{\partial x \partial y} \right)_{i,j} = \frac{\bar{T}_{i+1,j+1} - 2\bar{T}_{i+1,j-1} - \bar{T}_{i-1,j+1} + \bar{T}_{i-1,j-1}}{4\Delta x \Delta y}$$

Proceeding in a similar manner, the central difference approximation to the third derivative is found to be

$$\left( \frac{\partial^3 \bar{T}}{\partial x^3} \right)_{i,j} = \frac{\bar{T}_{i+2,j} - 2\bar{T}_{i+1,j} + 2\bar{T}_{i-1,j} - \bar{T}_{i-2,j}}{2\Delta x^3}.$$

Similar approximations can be obtained even to higher order derivatives.

## CHAPTER IV

### Finite Difference Solution of MHD Mixed Convection Flow through an Impulsively Started Permeable Vertical Plate with Diffusion-Thermo and Thermal-Diffusion Effects

#### 4.1. Mathematical Model of the Flow

An unsteady mixed convective heat and mass transfer flow of an electrically conducting incompressible viscous fluid through a porous medium along electrically non-conducting isothermal infinite impulsively stretched vertical porous plate with thermal diffusion and diffusion thermo effects have been considered. The positive  $x$  coordinate is measured along the plate in the direction of fluid motion and the positive  $y$  coordinate is measured normal to the plate. Initially, it is considered that the plate as well as the fluid is at the same temperature  $\bar{T}(=\bar{T}_\infty)$  and concentration  $\bar{C}(=\bar{C}_\infty)$ . Also it is assumed that the fluid and the plate is at rest. After that the plate is to be moving with a constant velocity  $U_0$  in its own plane. Instantaneously at time  $t > 0$ , the temperature of the plate and species concentration are raised to  $\bar{T}_w(>\bar{T}_\infty)$  and  $\bar{C}_w(>\bar{C}_\infty)$  respectively, which are there after maintained constant, where  $\bar{T}_w, \bar{C}_w$  are temperature and species concentration at the wall and  $\bar{T}_\infty, \bar{C}_\infty$  are the temperature and concentration of the species outside the plate respectively. The physical configuration of the problem is furnished in Figure 2.1

The imposed uniform magnetic field  $\mathbf{B}$  is taken as  $(0, B_0, 0)$ . The magnetic Reynolds number of the flow is taken to be small enough so that the induced magnetic field is negligible in comparison with applied magnetic field. The magnetic lines are fixed relative to the fluid. Using the relation  $\nabla \cdot \mathbf{J} = 0$  for the current density  $\mathbf{J} = (J_x, J_y, J_z)$ , where  $J_y = \text{constant}$ . Since the plate is non-conducting,  $J_y = 0$  at the plate and hence zero everywhere. The fluid is assumed to have constant properties except that the influence of the density variations with temperature and concentration, which are considered only in the body force term.

Within the framework of the above stated assumptions with reference to the generalized equations described in Chapter 2, the physical variables are functions of  $y$  and  $t$  only. Assuming that the Boussinesq and boundary-layer approximations hold and using the Darcy-Forchheimer model, the

equations governing the problem are (Alam and Rahman (1992)) governed by the following system of coupled non-linear partial differential equations (as stated in Chapter II):

**Continuity equation:**

$$\frac{\partial v}{\partial y} = 0 \quad (4.1)$$

**Momentum equation:**

$$\frac{\partial u}{\partial t} - v_0 \frac{\partial u}{\partial y} = \epsilon \frac{\partial^2 u}{\partial y^2} + g S_T (\bar{T} - \bar{T}_\infty) + g S_C (\bar{C} - \bar{C}_\infty) - \frac{\dagger B_0^2 u}{\dots} - \frac{\sim}{\dots k_1} u \quad (4.2)$$

**Concentration equation:**

$$\frac{\partial \bar{C}}{\partial t} - v_0 \frac{\partial \bar{C}}{\partial y} = D \frac{\partial^2 \bar{C}}{\partial y^2} + \frac{D k_t}{T_m} \frac{\partial^2 \bar{T}}{\partial y^2} \quad (4.3)$$

**Energy equation:**

$$\frac{\partial \bar{T}}{\partial t} - v_0 \frac{\partial \bar{T}}{\partial y} = \frac{1}{\dots c_p} \frac{\partial}{\partial y} \left( K(\bar{T}) \frac{\partial \bar{T}}{\partial y} \right) + \frac{D k_t}{c_s c_p} \frac{\partial^2 \bar{C}}{\partial y^2} + \frac{\dagger B_0^2 u^2}{\dots c_p} + \frac{\epsilon}{c_p} \left( \frac{\partial u}{\partial y} \right)^2 \quad (4.4)$$

The corresponding initial and boundary conditions are prescribed as follows:

$$t \leq 0, u = 0, \bar{C} \rightarrow \bar{C}_\infty, \bar{T} \rightarrow \bar{T}_\infty \text{ for all } y \quad (4.5)$$

$$t > 0, u = U_0, \bar{C} \rightarrow \bar{C}_w, \bar{T} \rightarrow \bar{T}_w \text{ at } y = 0$$

$$u \rightarrow 0, \bar{C} \rightarrow \bar{C}_\infty, \bar{T} \rightarrow \bar{T}_\infty \text{ as } y \rightarrow \infty \quad (4.6)$$

Here  $x, y$  are Cartesian coordinate system;  $u$  and  $v$  are the velocity components along and normal to the plate,  $\epsilon$  is the kinematic viscosity,  $\sim$  is the fluid viscosity and  $k_1$  is the permeability of the porous medium,  $g$  is the acceleration due to gravity,  $S_T$  is the thermal expansion coefficient,  $S_C$  and the concentration expansion coefficient,  $\dots$  is the density,  $D$  is the coefficient of mass diffusivity,  $k_t$  is the thermal diffusion ratio and  $T_m$  is the mean fluid temperature,  $c_p$  is the specific heat at the constant pressure,  $c_s$  is the concentration susceptibility and  $K(\bar{T}) = K_0 [1 + \chi_1 (\bar{T} - \bar{T}_\infty)]$  (Usman and Uwanta (2013)),  $K_0$  is the thermal conductivity of the ambient fluid.

## 4.2. Mathematical Formulation

Since the solutions of the governing equations (4.2) – (4.4) under the initial conditions (4.5) and boundary conditions (4.6) will be based on the Finite Difference Method it is required to make the equations dimensionless. For this purpose we will now introduce the following non-dimensional quantities:

$$Y = \frac{yU_0}{\epsilon}, U = \frac{u}{U_0}, \dagger = \frac{tU_0^2}{\epsilon}, \ddagger = \frac{tU_\infty^2}{\epsilon}, T = \frac{\bar{T} - \bar{T}_\infty}{\bar{T}_w - \bar{T}_\infty}, \bar{T} = \frac{T - T_\infty}{T_w - T_\infty}, C = \frac{\bar{C} - \bar{C}_\infty}{\bar{C}_w - \bar{C}_\infty}$$

From the above dimensionless variables, we have

$$u = U_0 U, \bar{C} = \bar{C}_\infty + (\bar{C}_w - \bar{C}_\infty) C \text{ and } \bar{T} = \bar{T}_\infty + (\bar{T}_w - \bar{T}_\infty) T, y = \frac{\epsilon Y}{U_0}, t = \frac{\epsilon \dagger}{U_0^2}.$$

Using these relations, we obtain the following derivatives

$$\begin{aligned} \frac{\partial u}{\partial t} &= \frac{U_0^3}{\epsilon} \frac{\partial U}{\partial \dagger}, \quad \frac{\partial u}{\partial y} = \frac{U_0^2}{\epsilon} \frac{\partial U}{\partial Y}, \quad \frac{\partial^2 u}{\partial y^2} = \frac{U_0^3}{\epsilon^2} \frac{\partial^2 U}{\partial Y^2}, \quad \frac{\partial \bar{C}}{\partial t} = \frac{U_0^2 (\bar{C}_w - \bar{C}_\infty)}{\epsilon} \frac{\partial C}{\partial \dagger}, \quad \frac{\partial \bar{C}}{\partial y} = \frac{U_0^2 (\bar{C}_w - \bar{C}_\infty)}{\epsilon} \frac{\partial C}{\partial Y}, \\ \frac{\partial^2 \bar{C}}{\partial y^2} &= \frac{U_0^2 (\bar{C}_w - \bar{C}_\infty)}{\epsilon^2} \frac{\partial^2 C}{\partial Y^2}, \quad \frac{\partial \bar{T}}{\partial t} = \frac{U_0^2 (\bar{T}_w - \bar{T}_\infty)}{\epsilon} \frac{\partial T}{\partial \dagger}, \quad \frac{\partial \bar{T}}{\partial y} = \frac{U_0^2 (\bar{T}_w - \bar{T}_\infty)}{\epsilon} \frac{\partial T}{\partial Y} \text{ and } \frac{\partial^2 \bar{T}}{\partial y^2} = \frac{U_0^2 (\bar{T}_w - \bar{T}_\infty)}{\epsilon^2} \frac{\partial^2 T}{\partial Y^2}. \end{aligned}$$

Now substitute the values of the above derivatives into the equations (4.2) – (4.4) together with the initial conditions (4.5) and boundary conditions (4.6), the following nonlinear coupled partial differential equations in terms of dimensionless variables are obtained

$$\begin{aligned} \frac{U_0^3}{\epsilon} \frac{\partial U}{\partial \dagger} - v_0 \frac{U_0^2}{\epsilon} \frac{\partial U}{\partial Y} &= \frac{U_0^3}{\epsilon} \frac{\partial^2 U}{\partial Y^2} - \frac{\dagger B_0^2 U U_0}{\dots} - \frac{\epsilon U U_0}{k} + g S T (\bar{T}_w - \bar{T}_\infty) + g S^* C (\bar{C}_w - \bar{C}_\infty) \\ \text{or, } \frac{\partial U}{\partial \dagger} - \frac{v_0}{U_0} \frac{\partial U}{\partial Y} &= \frac{\partial^2 U}{\partial Y^2} - \frac{\dagger B_0^2 \epsilon}{\dots U_0^2} - \frac{\epsilon^2}{U_0^2 k} + \frac{g S T (\bar{T}_w - \bar{T}_\infty) \epsilon}{U_0^3} + \frac{g S^* C (\bar{C}_w - \bar{C}_\infty) \epsilon}{U_0^3} \\ \text{or, } \frac{\partial U}{\partial \dagger} - \} \frac{\partial U}{\partial Y} &= \frac{\partial^2 U}{\partial Y^2} - M U - \chi U + Gr T + Gm C \end{aligned} \quad (4.7)$$

$$\begin{aligned} \frac{U_0^2 (\bar{C}_w - \bar{C}_\infty)}{\epsilon} \frac{\partial C}{\partial \dagger} - \frac{v_0 U_0}{\epsilon} \frac{\partial C}{\partial Y} (\bar{C}_w - \bar{C}_\infty) &= D \frac{U_0^2 (\bar{C}_w - \bar{C}_\infty)}{\epsilon^2} \frac{\partial^2 C}{\partial Y^2} + D_r \frac{U_0^2 (\bar{T}_w - \bar{T}_\infty)}{\epsilon^2} \frac{\partial^2 T}{\partial Y^2} \\ \text{or, } \frac{\partial C}{\partial \dagger} - \frac{v_0}{U_0} \frac{\partial C}{\partial Y} &= \frac{D}{\epsilon} \frac{\partial^2 C}{\partial Y^2} + \frac{D_r (\bar{T}_w - \bar{T}_\infty)}{\epsilon (\bar{C}_w - \bar{C}_\infty)} \frac{\partial^2 T}{\partial Y^2} \\ \text{or, } \frac{\partial C}{\partial \dagger} - \} \frac{\partial C}{\partial Y} &= \frac{1}{S c} \frac{\partial^2 C}{\partial Y^2} + S r \frac{\partial^2 T}{\partial Y^2} \end{aligned} \quad (4.8)$$



$$\begin{aligned}
& \frac{U_0^2(\bar{T}_w - \bar{T}_\infty)}{\epsilon} \frac{\partial T}{\partial \dagger} - \frac{v_0 U_0^2(\bar{T}_w - \bar{T}_\infty)}{\epsilon} \frac{\partial T}{\partial Y} = \frac{1}{\dots C_p} \frac{U_0^2(\bar{T}_w - \bar{T}_\infty)^2 K_0 \chi}{\epsilon^2} \left( \frac{\partial T}{\partial Y} \right)^2 + \frac{1}{\dots C_p} \frac{U_0^2(\bar{T}_w - \bar{T}_\infty) K(T)}{\epsilon^2} \frac{\partial^2 T}{\partial Y^2} \\
& \quad + \frac{D_M}{\dots C_p} \frac{U_0^2(\bar{C}_w - \bar{C}_\infty)}{\epsilon^2} \frac{\partial^2 C}{\partial Y^2} + b U_0^2 U^2 + \frac{1}{C_p} \frac{U_0^4}{\epsilon} \left( \frac{\partial U}{\partial Y} \right)^2 \\
\text{or, } & \frac{\partial T}{\partial \dagger} - \frac{v_0}{U_0} \frac{\partial T}{\partial Y} = \frac{1}{\dots C_p} \left[ \frac{(\bar{T}_w - \bar{T}_\infty) K_0 \chi}{\epsilon} \left( \frac{\partial T}{\partial Y} \right)^2 + \frac{K(T)}{\epsilon} \frac{\partial^2 T}{\partial Y^2} \right] + \frac{D_M}{\dots C_p \epsilon} \frac{(\bar{C}_w - \bar{C}_\infty)}{(\bar{T}_w - \bar{T}_\infty)} \frac{\partial^2 C}{\partial Y^2} + \frac{b \epsilon U^2}{(\bar{T}_w - \bar{T}_\infty)} \\
& \quad + \frac{U_0^2}{C_p (\bar{T}_w - \bar{T}_\infty)} \left( \frac{\partial U}{\partial Y} \right)^2 \\
\text{or, } & \frac{\partial T}{\partial \dagger} - \} \frac{\partial T}{\partial Y} = \frac{K_0}{\dots C_p \epsilon} \left[ \chi (\bar{T}_w - \bar{T}_\infty) \left( \frac{\partial T}{\partial Y} \right)^2 + (1 + \chi (\bar{T} - \bar{T})) \frac{\partial^2 T}{\partial Y^2} \right] + Du \frac{\partial^2 C}{\partial Y^2} + MEc U^2 + Ec \left( \frac{\partial U}{\partial Y} \right)^2 \\
\text{or, } & \frac{\partial T}{\partial \dagger} - \} \frac{\partial T}{\partial Y} = \frac{1}{Pr} \left[ \dagger \left( \frac{\partial T}{\partial Y} \right)^2 + (1 + \dagger) \frac{\partial^2 T}{\partial Y^2} \right] + Du \frac{\partial^2 C}{\partial Y^2} + MEc U^2 + Ec \left( \frac{\partial U}{\partial Y} \right)^2 \tag{4.9}
\end{aligned}$$

with the corresponding initial and boundary conditions are

$$\dagger = 0, U = 0, C = 0, T = 0 \text{ for all values of } Y \tag{4.10}$$

$$U = 1, C = 1, T = 1 \text{ at } Y = 0, \dagger > 0$$

$$U = 0, C \rightarrow 0, T \rightarrow 0 \text{ as } Y \rightarrow \infty, \dagger > 0 = 0, C \rightarrow 0, T \rightarrow 0 \text{ as } Y \rightarrow \infty, \dagger > 0 \tag{4.11}$$

where  $\dagger$  represents the dimensionless time,  $Y$  is the dimensionless Cartesian coordinate,  $U$  is the dimensionless primary velocity,  $T$  is the dimensionless temperature,  $C$  is the dimensionless concentration,

$$\} = \frac{v_0}{U_0} \text{ (Suction Parameter), } Gr = \frac{g S_T (\bar{T}_w - \bar{T}_\infty) \epsilon}{U_0^3} \text{ (Grashof Number),}$$

$$Gm = \frac{g S_c (\bar{C}_w - \bar{C}_\infty) \epsilon}{U_0^3} \text{ (Modified Grashof Number), } \chi = \frac{\sim \epsilon}{\dots k_1 U_0^2} \text{ (Permeability of the porous medium),}$$

$$M = \frac{\dagger B_0^2 \epsilon}{\dots U_0^2} \text{ (Magnetic Parameter), } Sc = \frac{\epsilon}{D} \text{ (Schmidt Number), and } Sr = \frac{Dk_T (\bar{T}_w - \bar{T}_\infty)}{\epsilon T_m (\bar{C}_w - \bar{C}_\infty)} \text{ (Soret}$$

$$\text{Number), } Pr = \frac{\dots c_p \epsilon}{K_0} \text{ (Prandtl Number), } \dagger = \chi_1 (\bar{T}_w - \bar{T}_\infty) \text{ (Variable thermal conductivity) (Usman and}$$

$$\text{Uwanta (2013)), } Du = \frac{Dk_t (\bar{C}_w - \bar{C}_\infty)}{\dots c_s c_p (\bar{T}_w - \bar{T}_\infty)} \text{ (Dufour Number) and } Ec = \frac{U_0^2}{c_p (\bar{T}_w - \bar{T}_\infty)} \text{ (Eckert Number)}$$

### 4.3. Numerical Solution

In this section, we attempt to solve the governing second order nonlinear coupled dimensionless partial differential equations with the associated initial and boundary conditions. For solving a transient free convection flow with mass transfer past a semi-infinite plate, Callahan and Marner (1976) used the explicit Finite Difference Method which is conditionally stable. On the contrary, the same problem was studied by Soundalgekar and Ganesan (1980) by an implicit Finite Difference Method which is unconditionally stable. The only difference between the two methods is that the implicit method being unconditionally stable is less expansive from the point of view of computer time. However, these two methods respectively employed by Callahan and Marner (1976) and Soundalgekar and Ganesan (1980), respectively produced the same results.

From the concept of the above discussion, for simplicity the Finite Difference Method has been used to solve equations (4.7) – (4.9) subject to the conditions given by (4.10) and (4.11). To solve the non-dimensional system by the finite difference technique, it is required a set of finite difference equations. In this case, the region within on the boundary layer is divided by some perpendicular lines of  $Y$ -axis, where  $Y$ -axis is normal to the medium as shown in Figure 4. It is assumed that the maximum length of boundary layer is  $Y_{\max} = (25)$  as corresponds to  $Y \rightarrow \infty$  i.e.  $Y$  varies from 0 to 25 and the number of grid spacing in  $Y$  directions is  $\bar{p}(=400)$ , hence the constant mesh size along  $Y$  axis becomes  $\Delta Y = 0.0625(0 \leq Y \leq 25)$  with a smaller time-step  $\Delta t = 0.001$ .

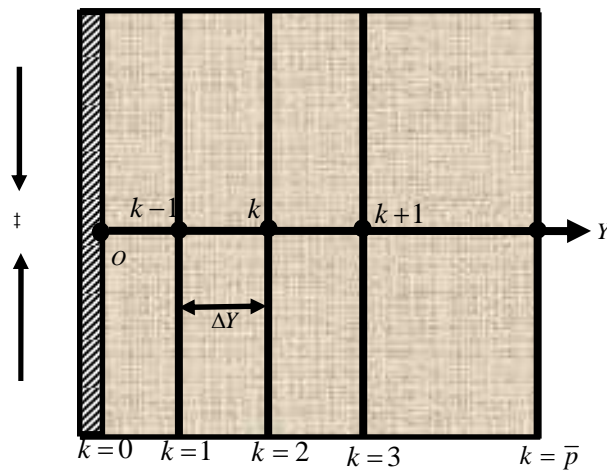


**Figure 4.3.1:** Implicit finite difference system grid.

Let  $U^{\bar{n}}$ ,  $C^{\bar{n}}$  and  $T^{\bar{n}}$  denote the values of  $U$ ,  $C$  and  $T$  at the end of a time-step respectively. Using the implicit finite difference approximation, the following relations are obtained as;

$$\begin{aligned} \left(\frac{\partial U}{\partial \dagger}\right)_k &= \frac{U_k^{\bar{n}+1} - U_k^{\bar{n}}}{\Delta \dagger}, \quad \left(\frac{\partial U}{\partial Y}\right)_k = \frac{U_{k+1}^{\bar{n}} - U_k^{\bar{n}}}{\Delta Y}, \quad \left(\frac{\partial^2 U}{\partial Y^2}\right)_k = \frac{U_{k+1}^{\bar{n}} - 2U_k^{\bar{n}} + U_{k-1}^{\bar{n}}}{(\Delta Y)^2}, \quad \left(\frac{\partial C}{\partial \dagger}\right)_k = \frac{C_k^{\bar{n}+1} - C_k^{\bar{n}}}{\Delta \dagger}, \\ \left(\frac{\partial C}{\partial Y}\right)_k &= \frac{C_{k+1}^{\bar{n}} - C_k^{\bar{n}}}{\Delta Y}, \quad \left(\frac{\partial^2 C}{\partial Y^2}\right)_k = \frac{C_{k+1}^{\bar{n}} - 2C_k^{\bar{n}} + C_{k-1}^{\bar{n}}}{(\Delta Y)^2}, \quad \left(\frac{\partial T}{\partial \dagger}\right)_k = \frac{T_k^{\bar{n}+1} - T_k^{\bar{n}}}{\Delta \dagger}, \quad \left(\frac{\partial T}{\partial Y}\right)_k = \frac{T_{k+1}^{\bar{n}} - T_k^{\bar{n}}}{\Delta Y} \quad \text{and} \\ \left(\frac{\partial^2 T}{\partial Y^2}\right)_k &= \frac{T_{k+1}^{\bar{n}} - 2T_k^{\bar{n}} + T_{k-1}^{\bar{n}}}{(\Delta Y)^2}. \end{aligned}$$

Substituting above values into equations (4.7) – (4.9), we obtain

$$\frac{U_k^{\bar{n}+1} - U_k^{\bar{n}}}{\Delta \dagger} - \left\} \frac{U_{k+1}^{\bar{n}} - U_k^{\bar{n}}}{\Delta Y} = \frac{U_{k+1}^{\bar{n}} - 2U_k^{\bar{n}} + U_{k-1}^{\bar{n}}}{(\Delta Y)^2} - MU_k^{\bar{n}} - \chi U_k^{\bar{n}} + Gr\bar{T}_k^{\bar{n}} + Gm\bar{C}_k^{\bar{n}} \quad (4.12)$$

$$\frac{C_k^{\bar{n}+1} - C_k^{\bar{n}}}{\Delta \dagger} - \left\} \frac{C_{k+1}^{\bar{n}} - C_k^{\bar{n}}}{\Delta Y} = \frac{1}{Sc} \frac{C_{k+1}^{\bar{n}} - 2C_k^{\bar{n}} + C_{k-1}^{\bar{n}}}{(\Delta Y)^2} + Sr \frac{T_{k+1}^{\bar{n}} - 2T_k^{\bar{n}} + T_{k-1}^{\bar{n}}}{(\Delta Y)^2} \quad (4.13)$$

$$\begin{aligned} \frac{T_k^{\bar{n}+1} - T_k^{\bar{n}}}{\Delta \dagger} - \left\} \frac{T_{k+1}^{\bar{n}} - T_k^{\bar{n}}}{\Delta Y} &= \frac{1}{Pr} \left[ \dagger \left( \frac{T_{k+1}^{\bar{n}} - T_k^{\bar{n}}}{\Delta Y} \right)^2 + (1 + \dagger) \frac{\bar{T}_{k+1}^{\bar{n}} - 2\bar{T}_k^{\bar{n}} + \bar{T}_{k-1}^{\bar{n}}}{(\Delta Y)^2} \right] \\ &+ Du \frac{C_{k+1}^{\bar{n}} - 2C_k^{\bar{n}} + C_{k-1}^{\bar{n}}}{(\Delta Y)^2} + MEc(U_k^{\bar{n}})^2 + Ec \left( \frac{U_{k+1}^{\bar{n}} - U_k^{\bar{n}}}{\Delta Y} \right)^2 \end{aligned} \quad (4.14)$$

with the corresponding initial and boundary conditions are

$$U_0^0 = 0, C_0^0 = 0, T_0^0 = 0 \quad (4.15)$$

$$U_0^{\bar{n}} = 1, C_0^{\bar{n}} = 1, T_0^{\bar{n}} = 1 \quad (4.16)$$

$$U_L^{\bar{n}} = 0, C_L^{\bar{n}} = 0, T_L^{\bar{n}} = 0 \quad \text{where } L \rightarrow \infty$$

Here the subscript  $k$  designates the grid points with  $Y$  coordinate and the superscript  $\bar{n}$  represents a value of time,  $\dagger = \bar{n}\Delta \dagger$ , where  $\bar{n} = 0, 1, 2, \dots$ . The velocity ( $U$ ), concentration ( $C$ ) and temperature ( $T$ ) distributions at all interior nodal points may be computed by successive applications of the above finite difference equations. The obtained values are graphically shown in Figures 4.1– 4.35.

#### 4.4. Results and Discussion

To obtain the steady-state solutions, the computations have been carried out up to dimensionless time  $\dagger = 50$ . Figure 4.1 represents the velocity profiles at several times. The area enclosed by a curve with both axes are represented by

$$U_A = \int_0^{25} U dY \quad (4.17)$$

Similarly for concentration and temperature profile it can be write as:

$$C_A = \int_0^{25} C dY \quad (4.18)$$

$$T_A = \int_0^{25} T dY \quad (4.19)$$

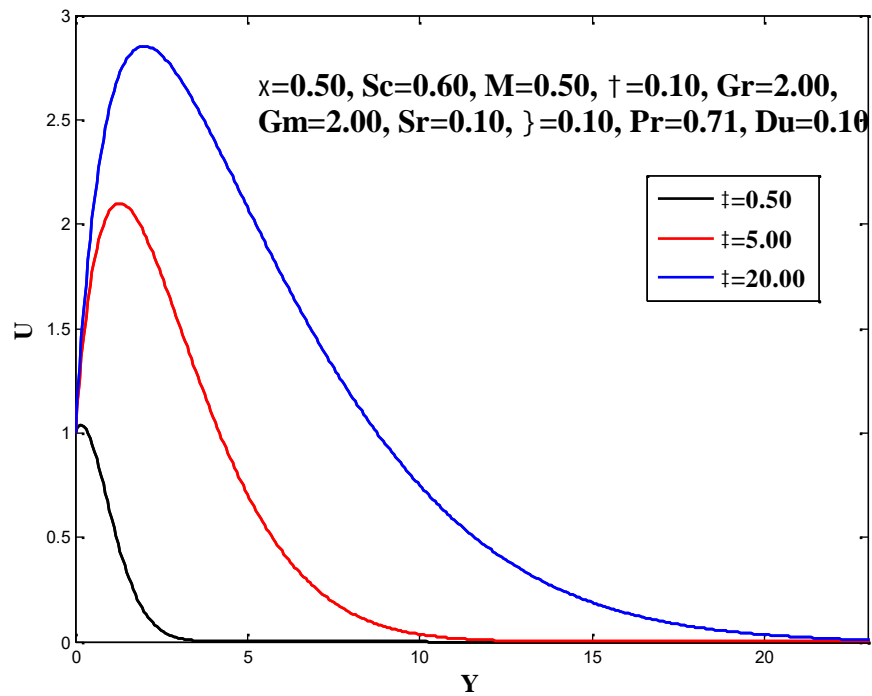


**Figure 4.1:** Velocity profiles for various values of dimensionless time,  $\dagger$ .

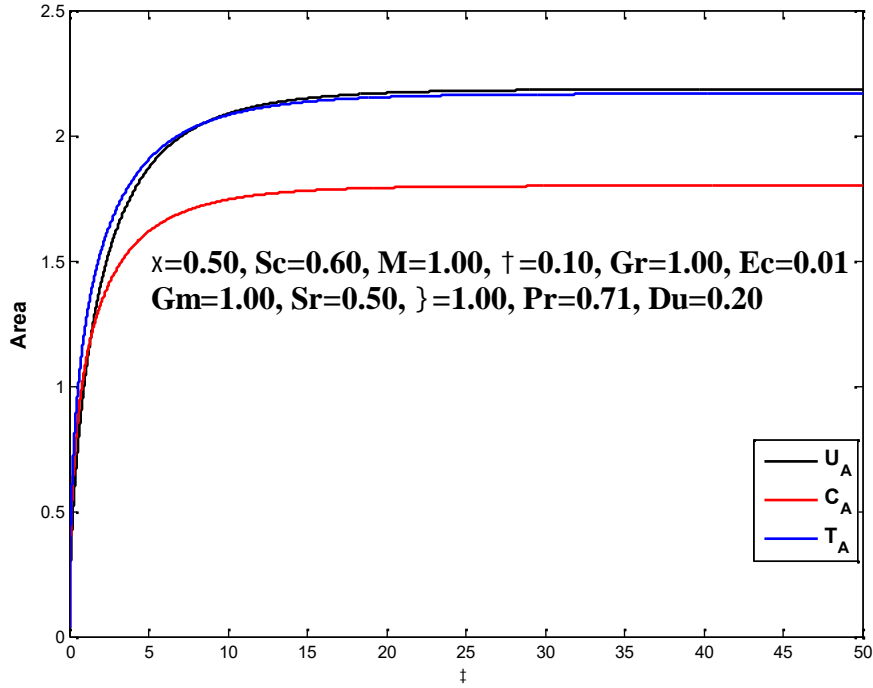


**Figure 4.2:** Area against dimensionless time,  $\dagger$  .

Figure 4.2 shows effects of the areas versus dimensionless time. In this figure it can be concluded that the results of the computations show little changes in the above mentioned quantities after dimensionless time,  $\dagger = 20$ . Thus, the solutions for dimensionless time,  $\dagger = 20$  are essentially steady-state solutions. To observe the physical situation of the problem, the steady-state solutions have been illustrated in Figures 4.3 – 4.35.

The influence of Grashof number  $Gr$  on the velocity, temperature and concentration distributions are presented in Figures 4.3 – 4.5. It is observed that velocity and temperature profiles are increasing with the increase of  $Gr$  but no remarkable effect of  $Gr$  on the concentration distributions is found. The effects of Modified Grashof number  $Gm$  on the velocity, temperature and concentration distributions are shown in Figures 4.6 – 4.8. It is observed that velocity and temperature profiles are increasing with the rise of  $Gm$ . But the concentration profiles are found decreasing a little with the increase of  $Gm$  close to the plate and a reverse effect is observed far away before asymptotically approaches to zero. The effects of Prandtl number  $Pr$  on the velocity, temperature and concentration distributions are presented in Figures 4.9 – 4.11. It is shown that velocity and temperature profiles are decreasing with

the increase of  $Pr$ . There is no significant effect of  $Pr$  on the concentration distributions as to be shown. The influence of Dufour number  $Du$  on the velocity, temperature and concentration distributions are presented in Figures 4.12 – 4.14. It is observed that velocity and temperature profiles show increasing effect with the increase of  $Du$ . No remarkable effect of  $Du$  on the concentration distributions is observed here. The effect of Schmidt number  $Sc$  on the velocity, temperature and concentration distributions are presented in Figures 4.15 – 4.17. It is observed that velocity, temperature and concentration profiles are decreasing with the increase of  $Sc$ . The influence of Soret number  $Sr$  on the velocity, temperature distributions and concentration distributions are discussed in Figures. 4.18 – 4.20. It is observed that velocity, temperature and concentration profiles show increasing behaviour with the increase of  $Sr$ .

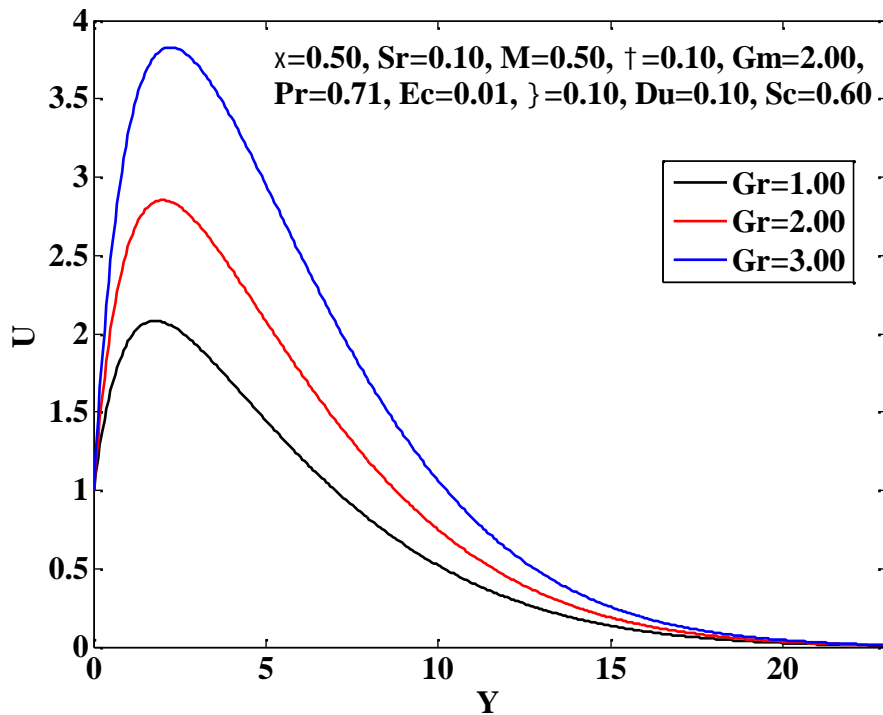


**Figure 4.3:** Velocity profiles for various values of Grashof Number,  $Gr$ .

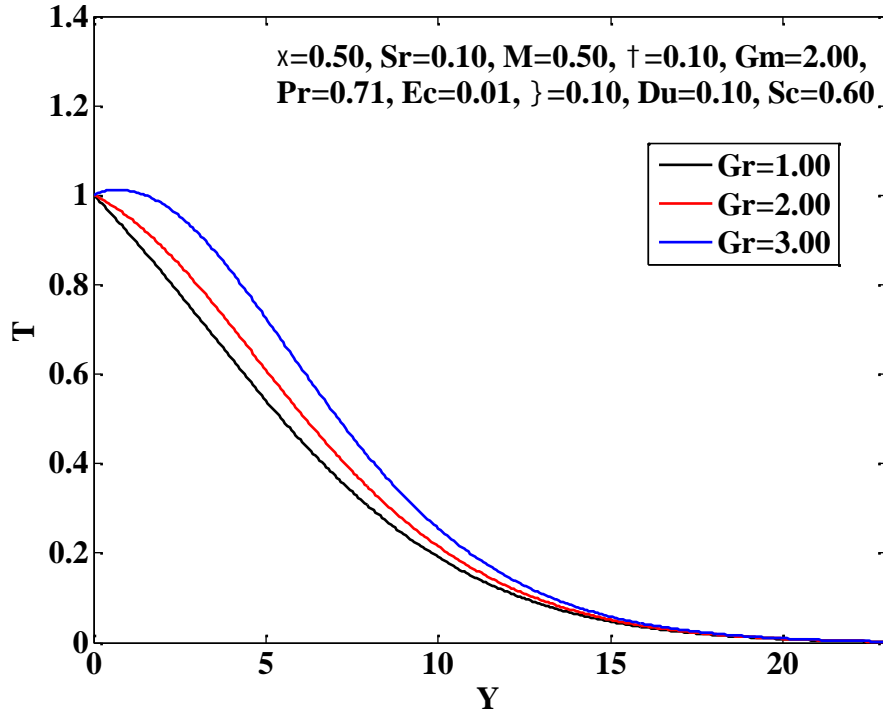


**Figure 4.4:** Temperature profiles for various values of Grashof Number,  $Gr$ .

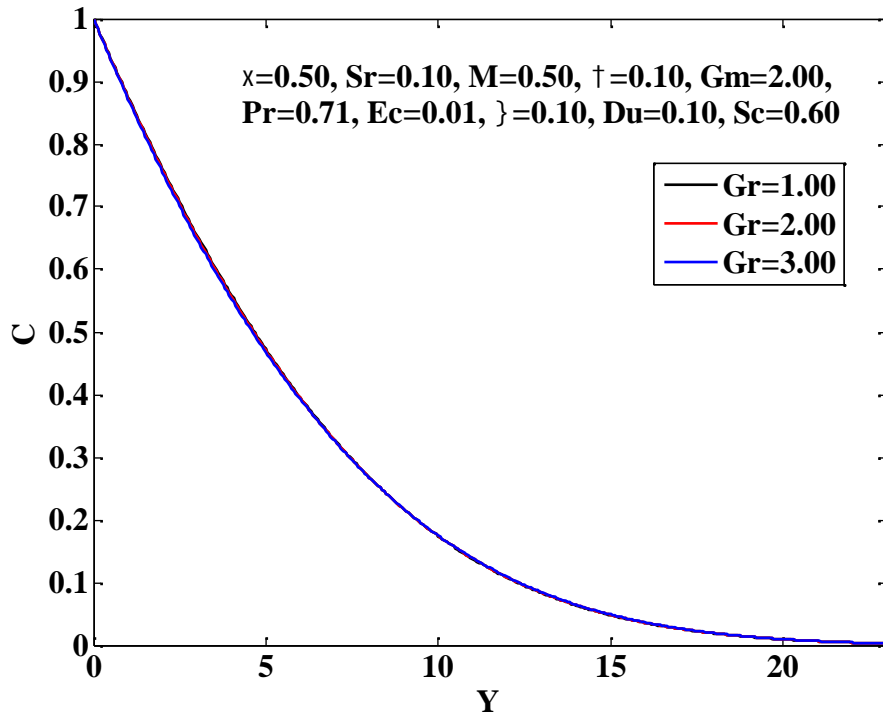


**Figure 4.5:** Concentration profiles for various values of Grashof Number,  $Gr$ .

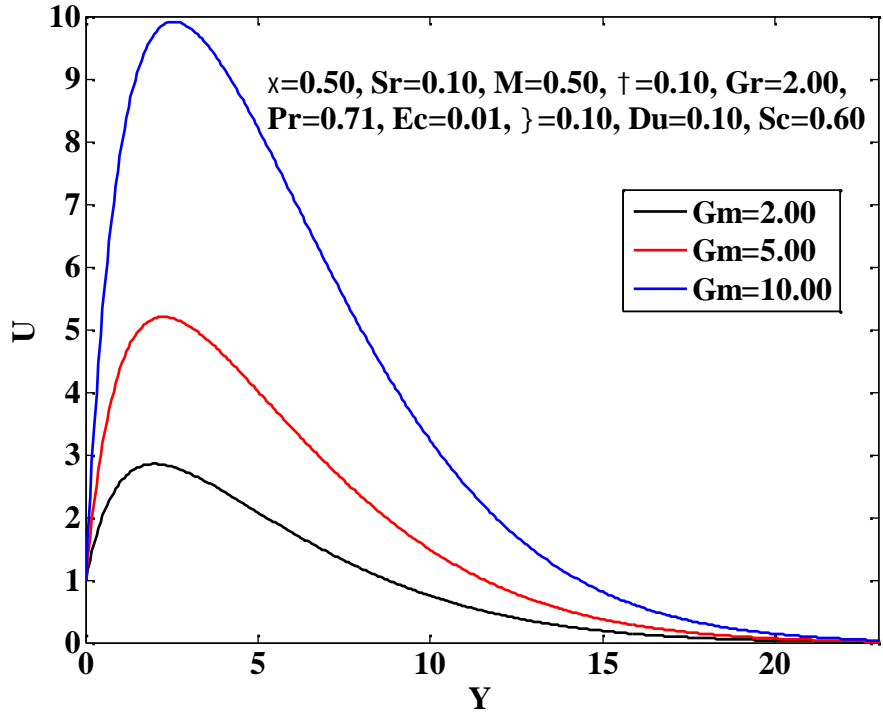


**Figure 4.6:** Velocity profiles for various values of Modified Grashof Number,  $Gm$ .

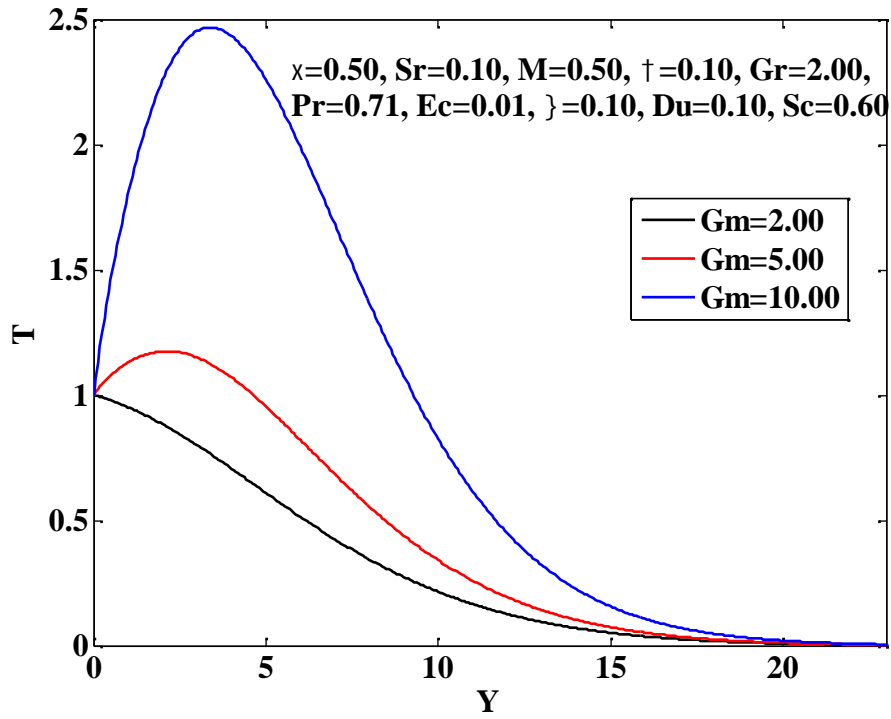


**Figure 4.7:** Temperature profiles for various values of Modified Grashof Number,  $Gm$ .



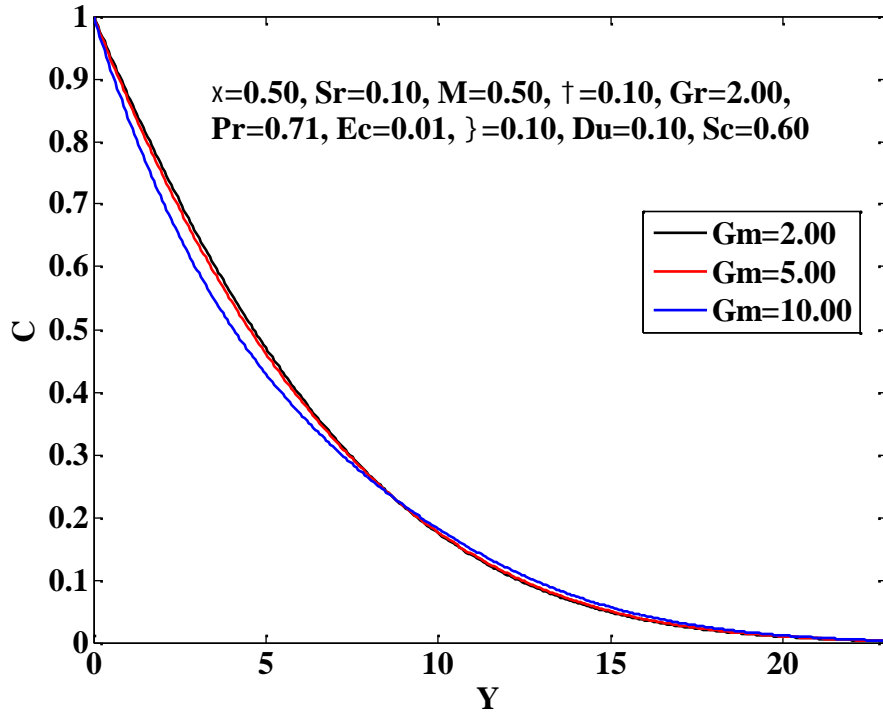


**Figure 4.8:** Concentration profiles for various values of Modified Grashof Number,  $Gm$ .

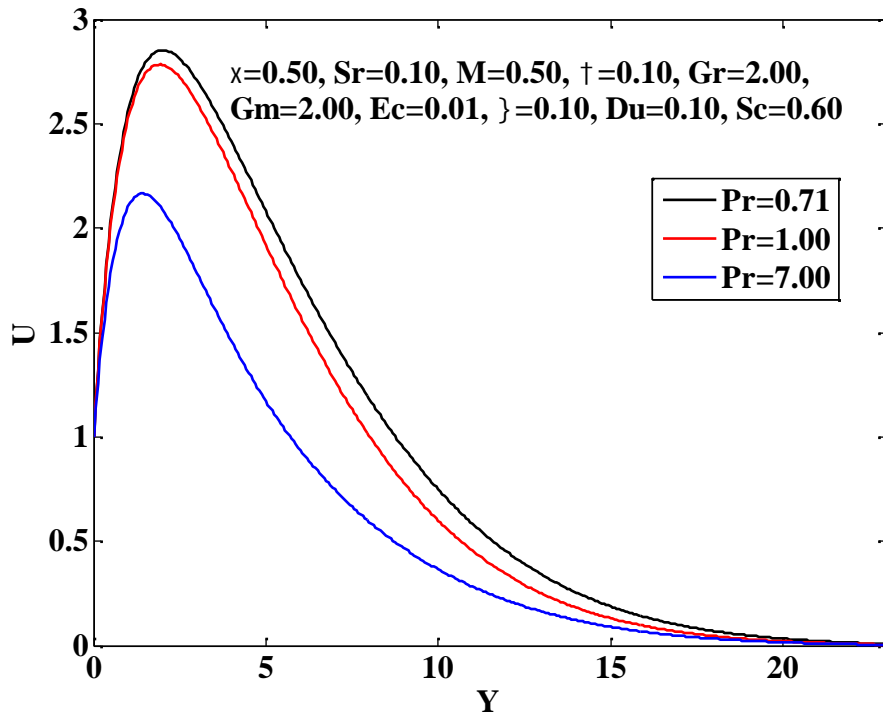


**Figure 4.9:** Velocity profiles for various values of Prandtl Number,  $Pr$ .

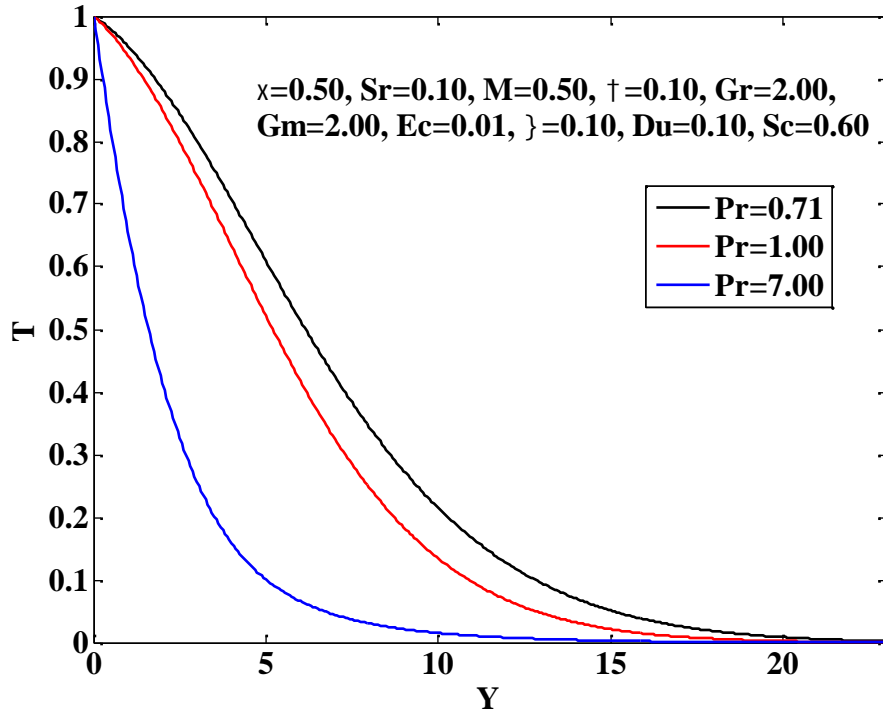


**Figure 4.10:** Temperature profiles for various values of Prandtl Number, Pr .

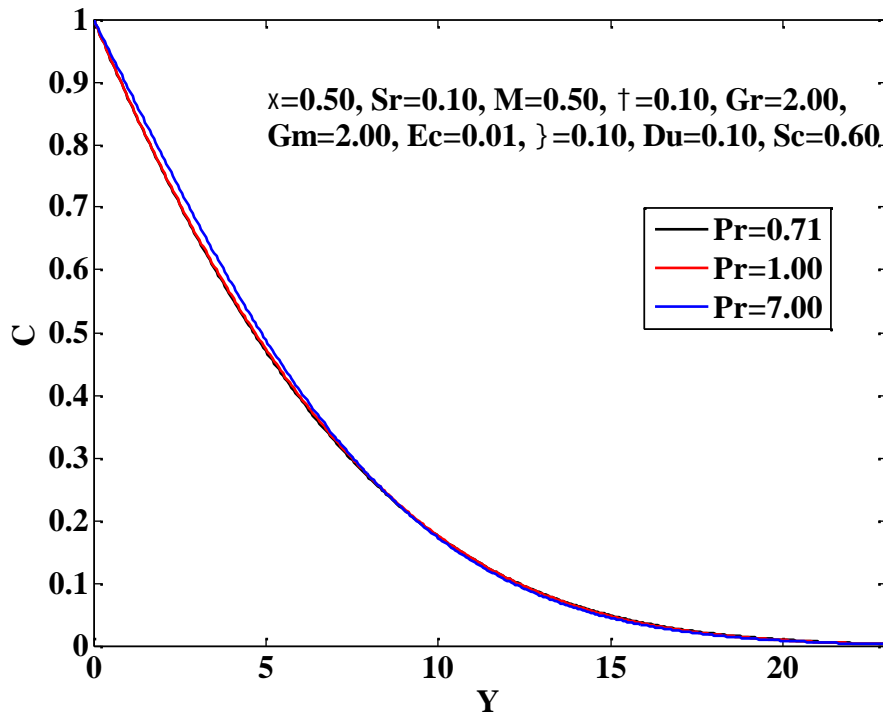


**Figure 4.11:** Concentration profiles for various values of Prandtl Number, Pr .

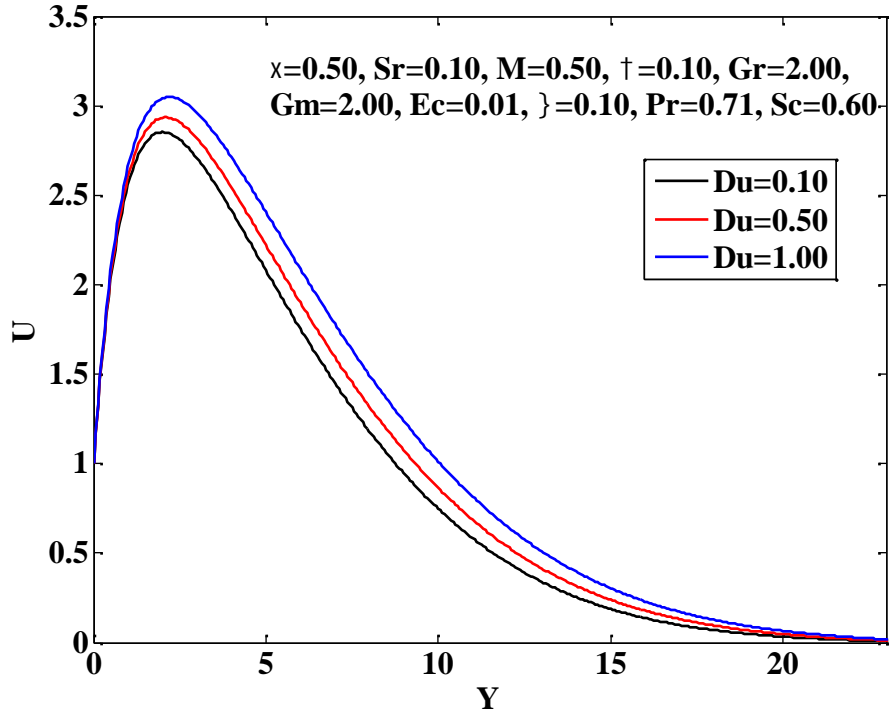


Figure 4.12: Velocity profiles for various values of Dufour Number,  $Du$ .

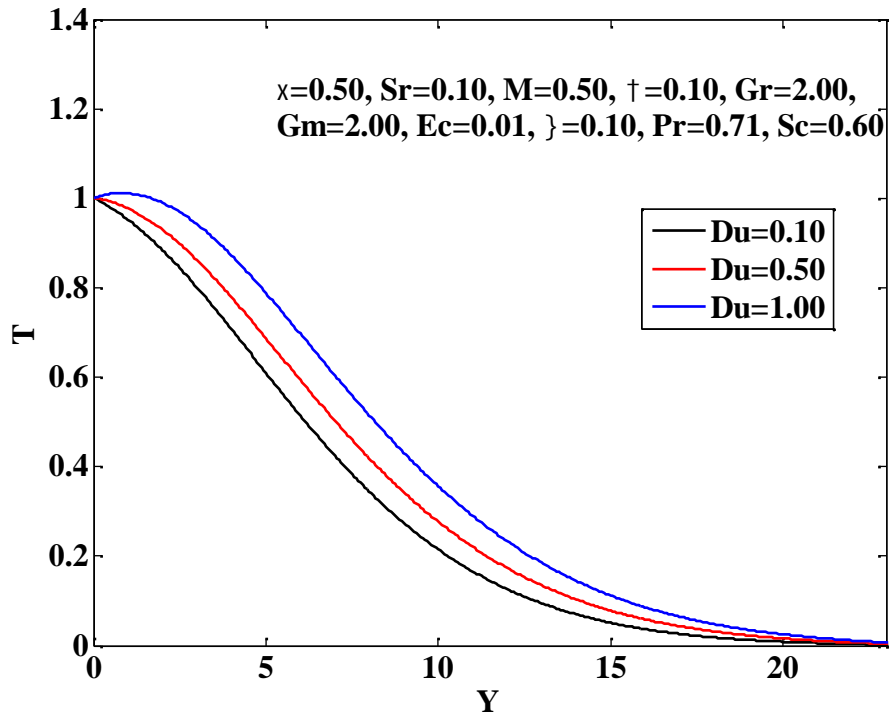
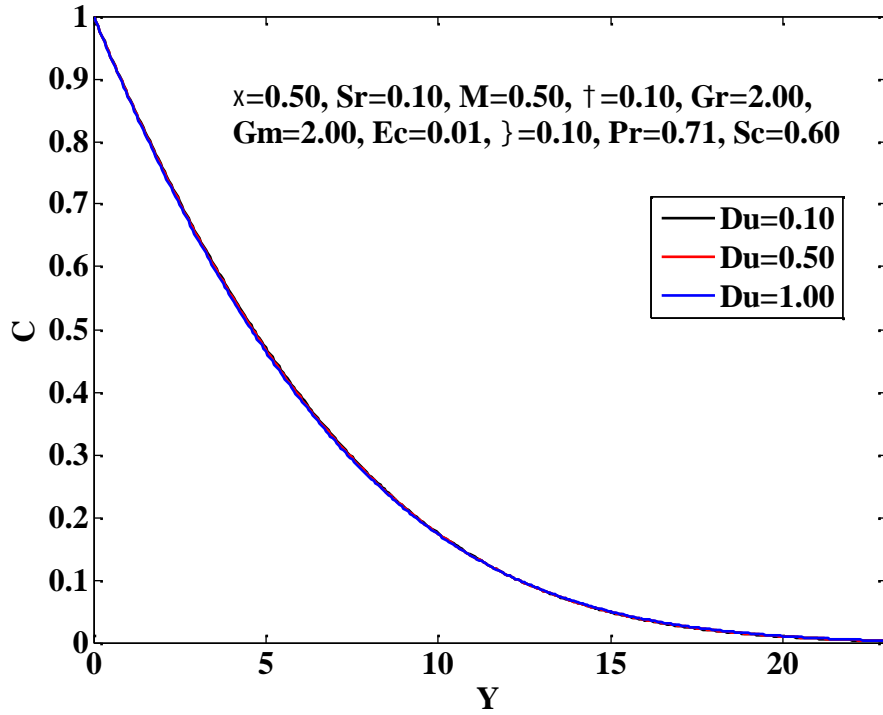
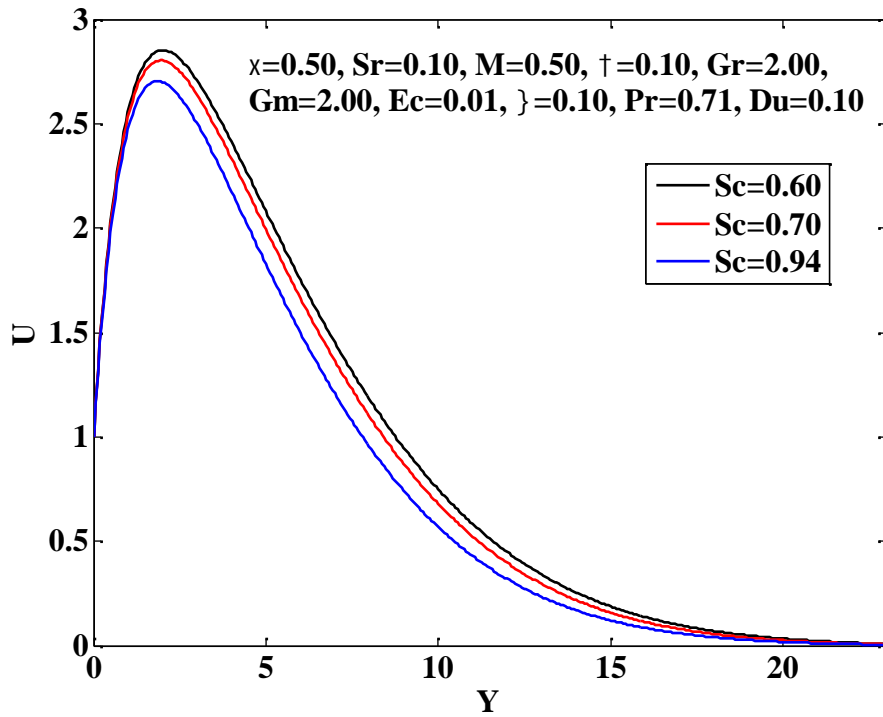


Figure 4.13: Temperature profiles for various values of Dufour Number,  $Du$ .



**Figure 4.14:** Concentration profiles for various values of Dufour Number,  $Du$ .



**Figure 4.15:** Velocity profiles for various values of Schmidt Number,  $Sc$ .

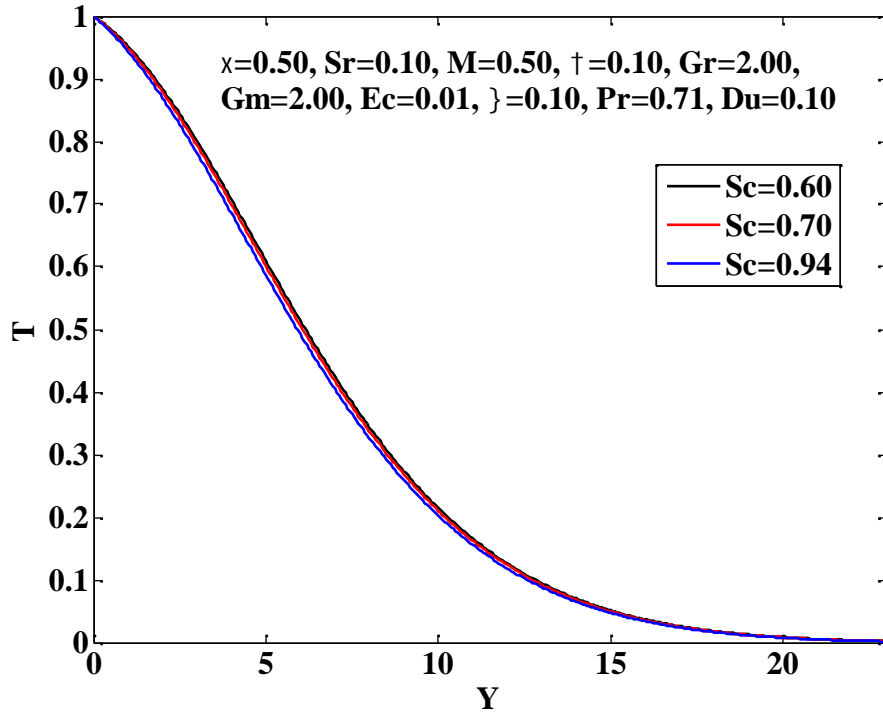


**Figure 4.16:** Temperature profiles for various values of Schmidt Number,  $Sc$ .

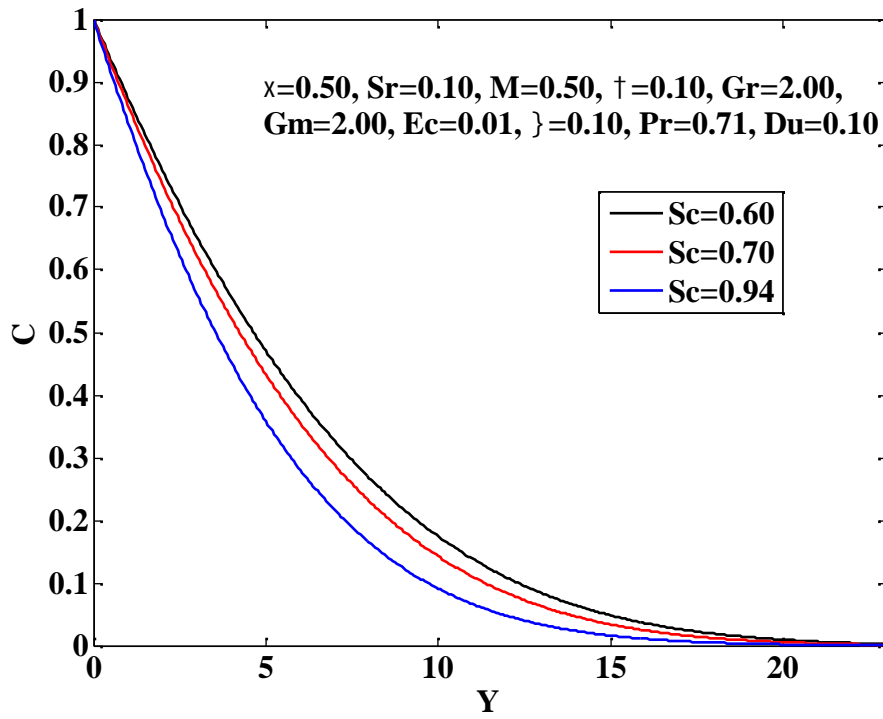


**Figure 4.17:** Concentration profiles for various values of Schmidt Number,  $Sc$ .

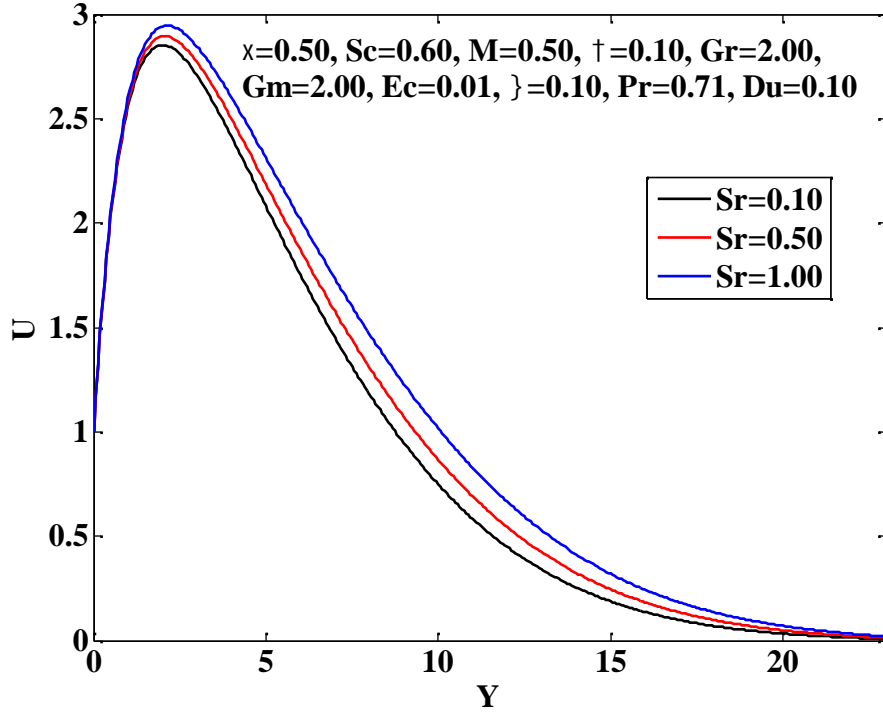


**Figure 4.18:** Velocity profiles for various values of Soret Number,  $Sr$ .

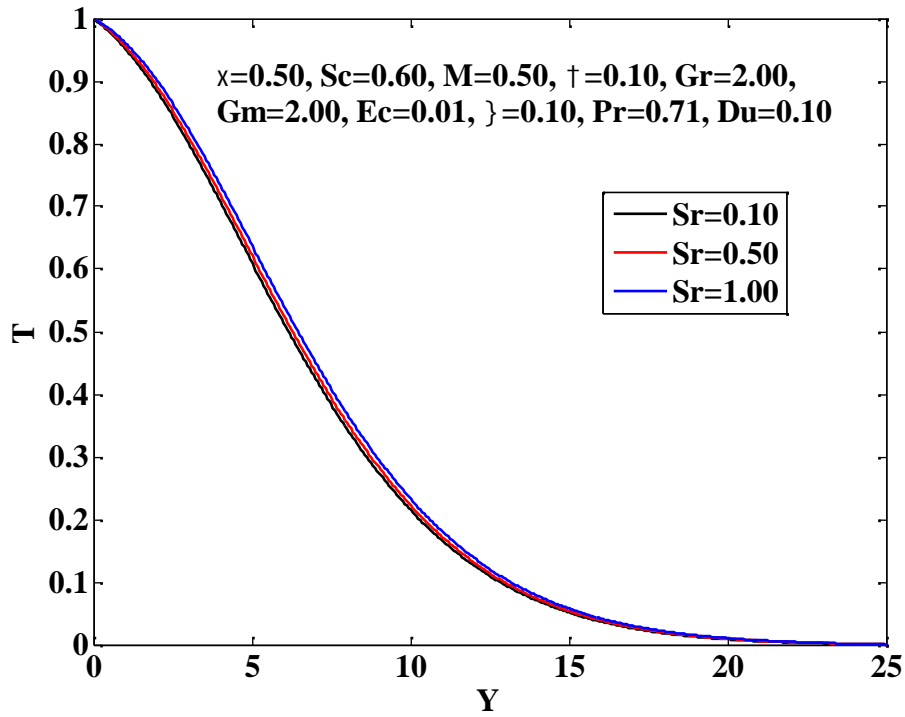


**Figure 4.19:** Temperature profiles for various values of Soret Number,  $Sr$ .

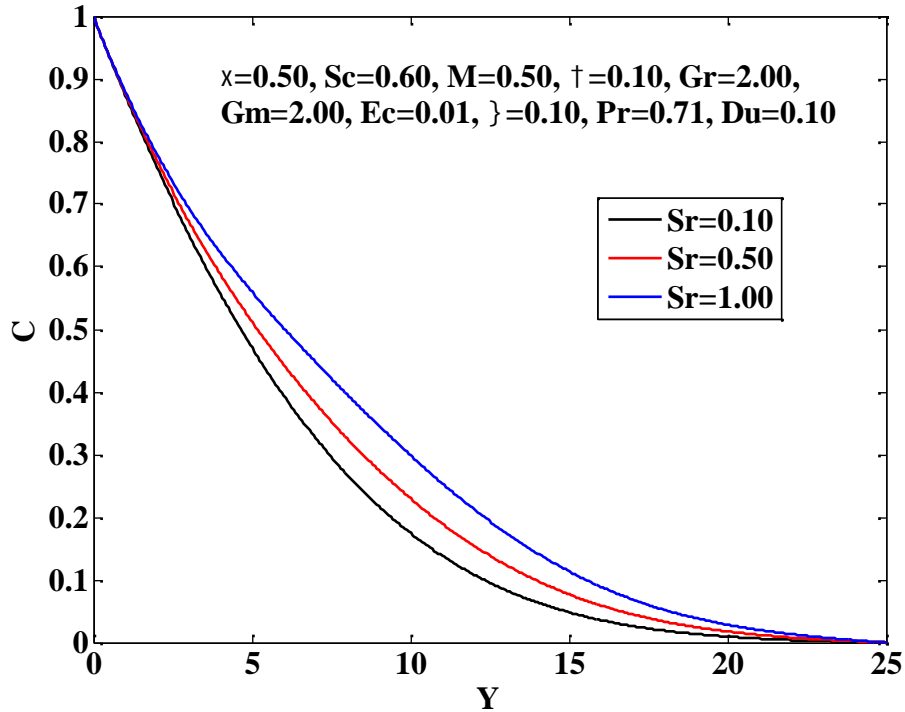


**Figure 4.20:** Concentration profiles for various values of Soret Number,  $Sr$ .

The effect of Magnetic parameter  $M$  on the velocity, temperature and concentration distributions are presented in Figures 4.21 – 4.23. It is observed that velocity and temperature profiles show decreasing effect with the rise of  $M$ . It is clearly seen from Figure 4.21 that the effects of increasing the magnetic field strength on the momentum boundary layer thickness leads to a decrease in the velocity width. It is due to the fact that a strong magnetic field results in a large damping effect on the velocity by creating a drag force that opposes the fluid motion. The effect Permeability of the porous medium  $\chi$  on the velocity, temperature and concentration distributions are presented in Figures 4.24 – 4.26. It is shown that velocity and temperature profiles are increasing with the increase of  $\chi$ . But no remarkable effects of  $M$  and  $\chi$  on the concentration distributions are observed. The influence of Suction parameter,  $\sigma$  on the velocity, temperature and concentration distributions are described in Figures 4.27 – 4.29. It is observed that velocity, temperature and concentration profiles are decreased quickly with the increase of  $\sigma$ . The effect of Eckert number  $Ec$  on the velocity, temperature and concentration are presented in Figures 4.30 – 4.32. It is observed that velocity and temperature profiles are increased with the increase of  $Ec$ . There is a small decrease of concentration profiles with increasing  $Ec$ .

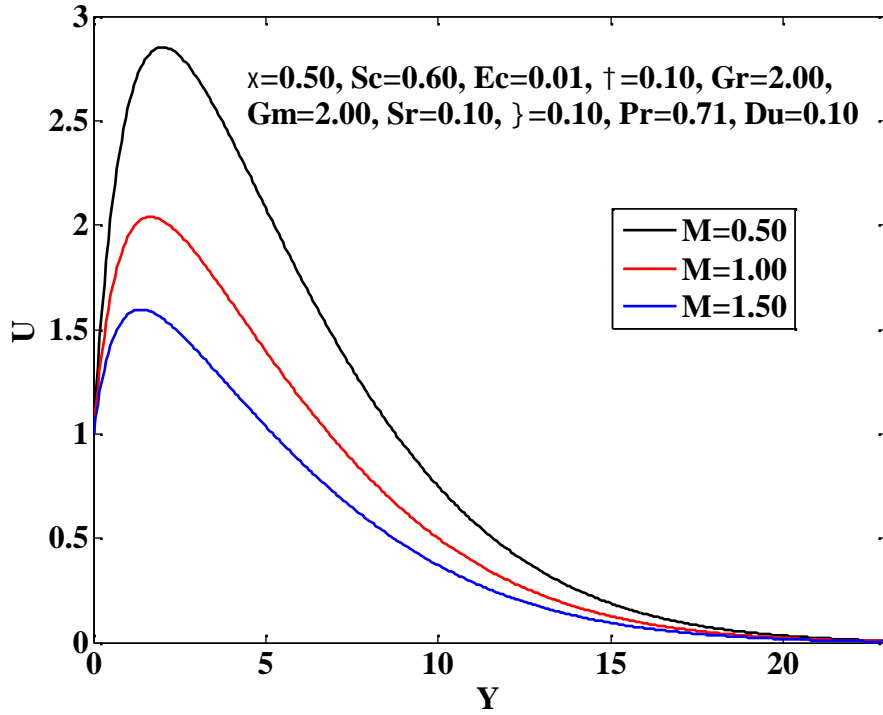


**Figure 4.21:** Velocity profiles for various values of Magnetic Parameter,  $M$ .

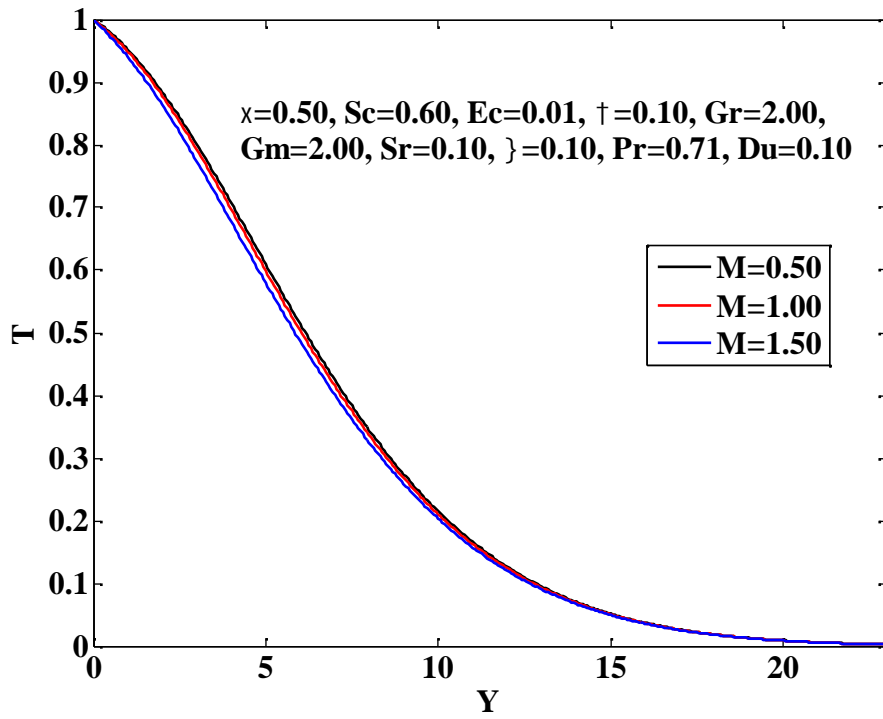


**Figure 4.22:** Temperature profiles for various values of Magnetic Parameter,  $M$ .



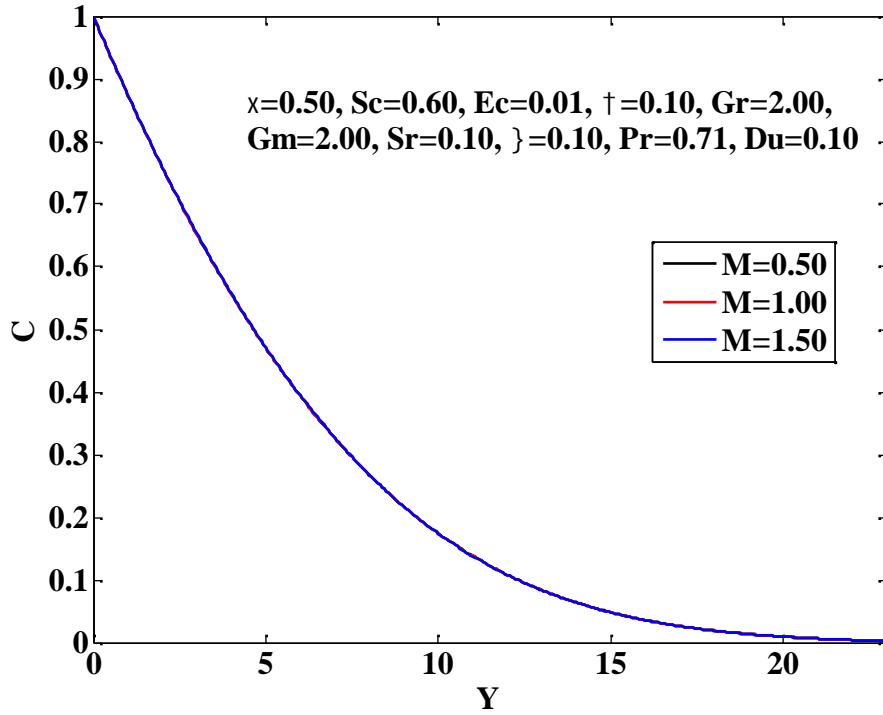


**Figure 4.23:** Concentration profiles for various values of Magnetic Parameter,  $M$  .

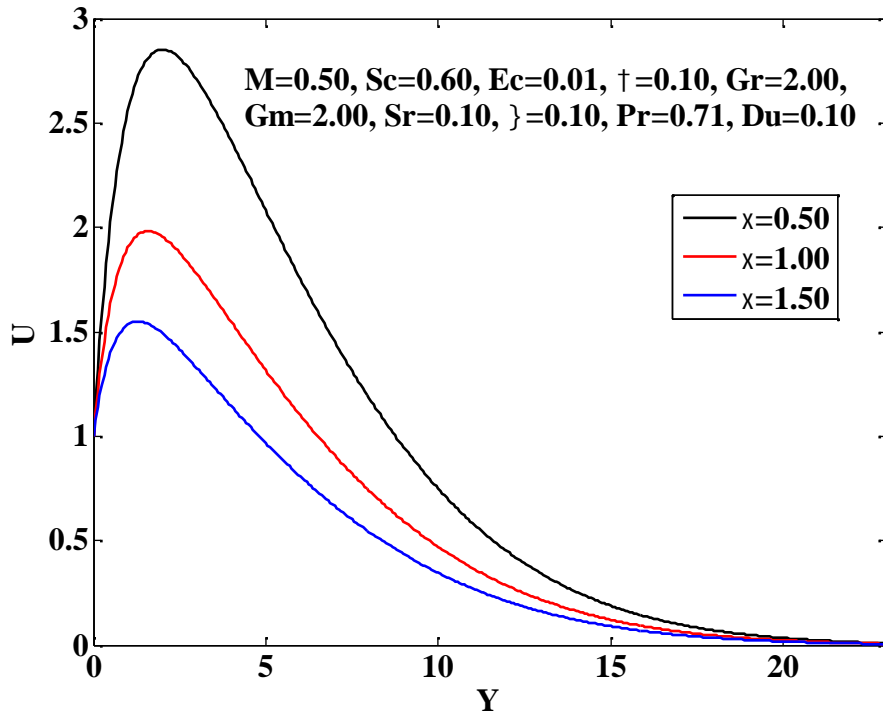


**Figure 4.24:** Velocity profiles for various values of Permeability of the porous medium,  $\chi$  .

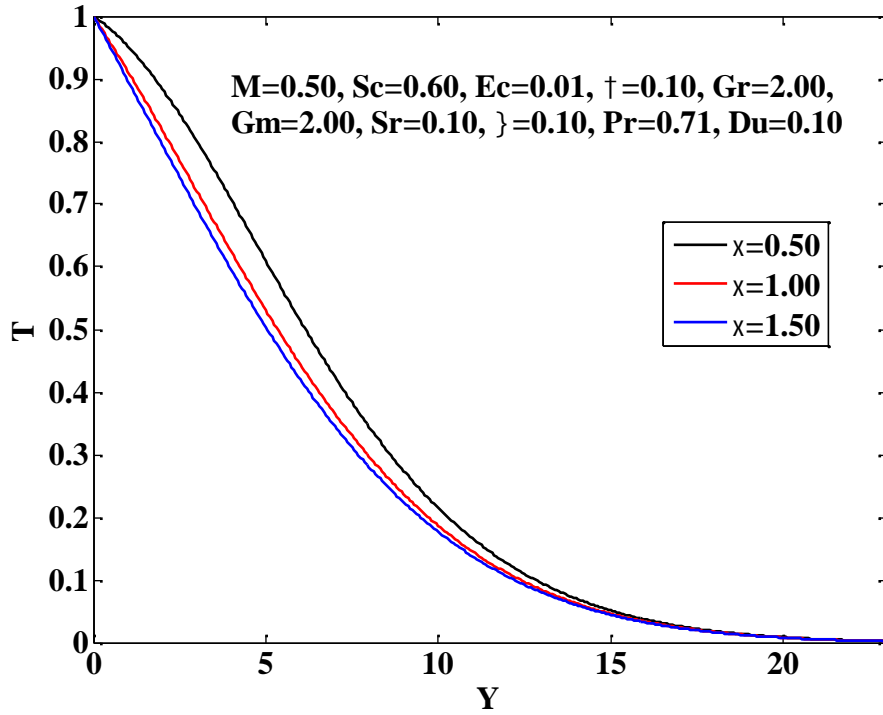


**Figure 4.25:** Temperature profiles for various values of Permeability of the porous medium,  $\chi$  .

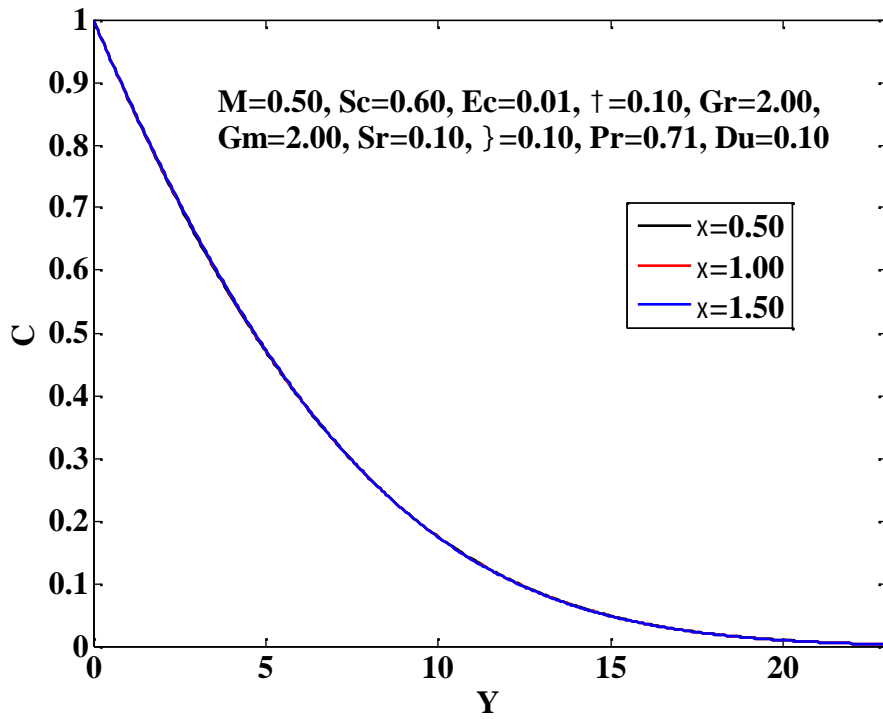


**Figure 4.26:** Concentration profiles for various values of Permeability of the porous medium,  $\chi$  .

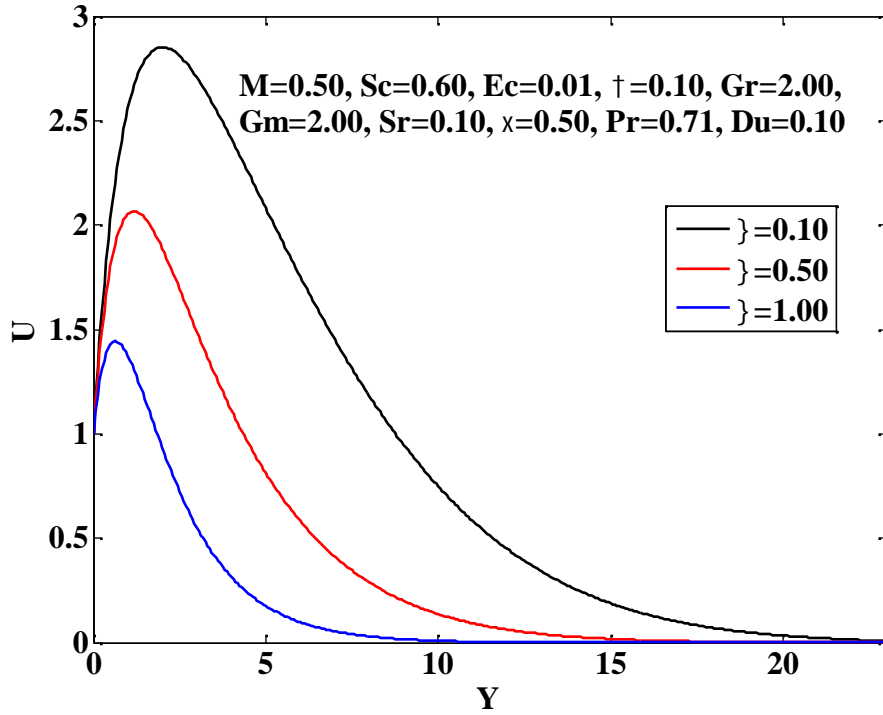


Figure 4.27: Velocity profiles for various values of Suction Parameter,  $\lambda$ .

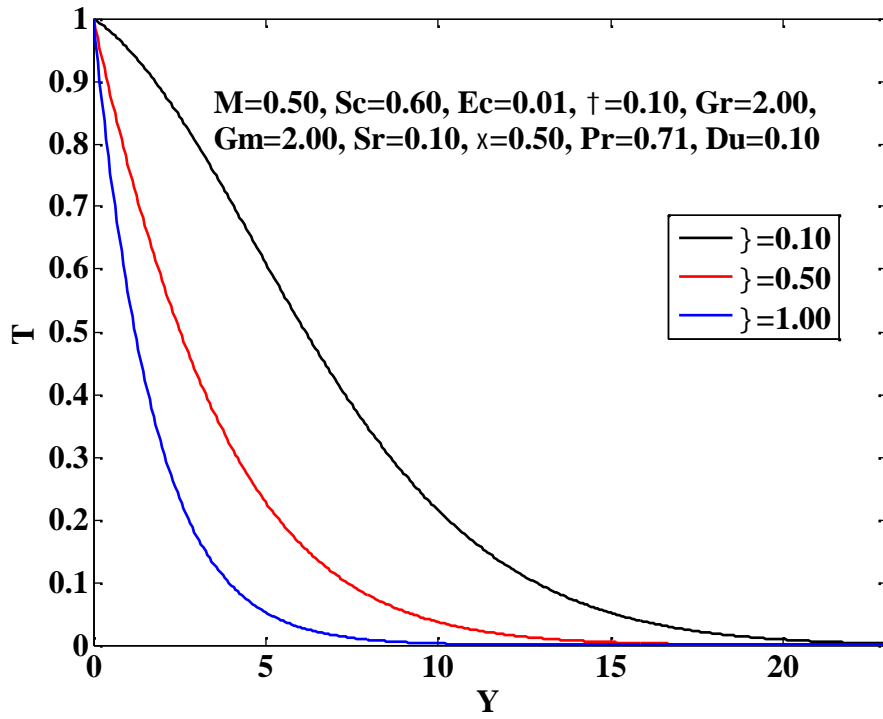


Figure 4.28: Temperature profiles for various values of Suction Parameter,  $\lambda$ .

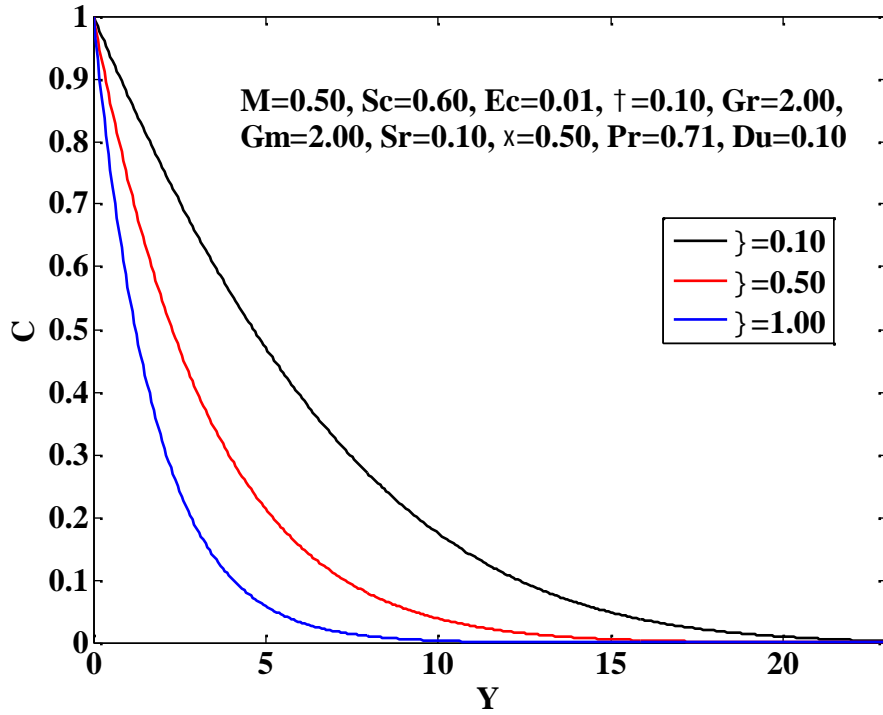


Figure 4.29: Concentration profiles for various values of Suction Parameter,  $\lambda$ .

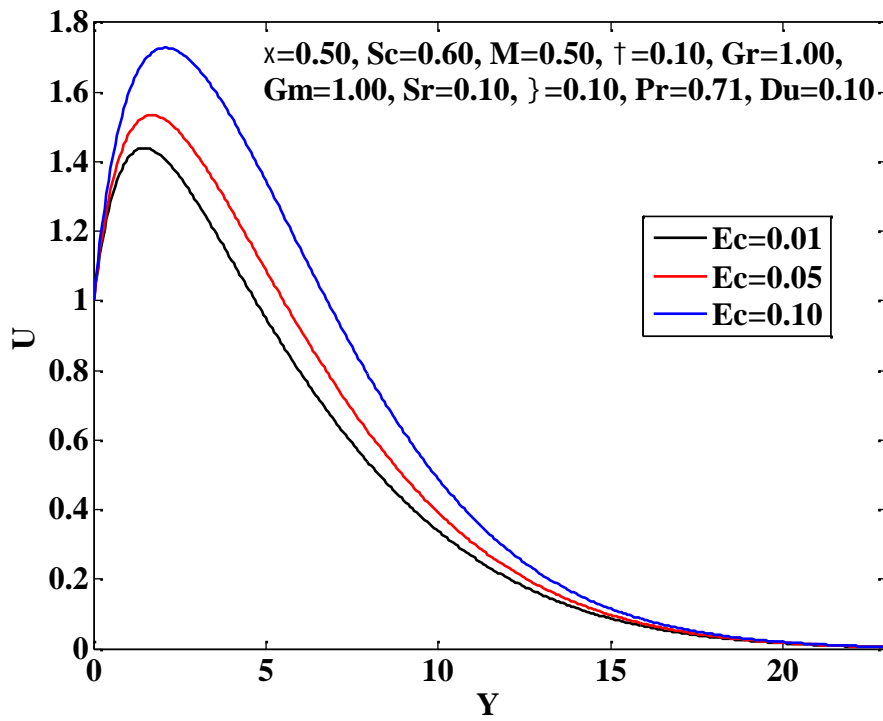
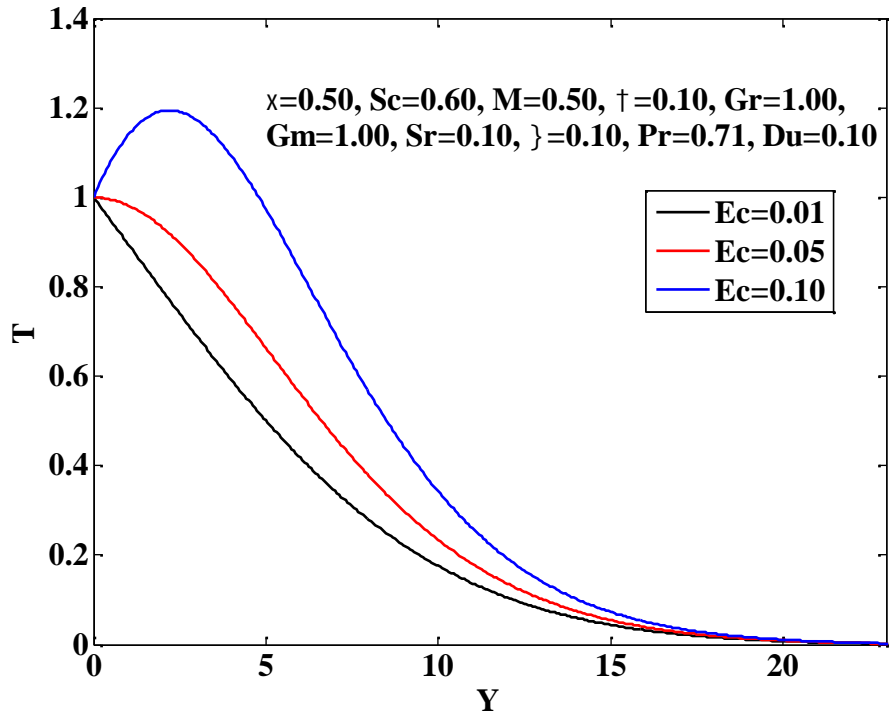
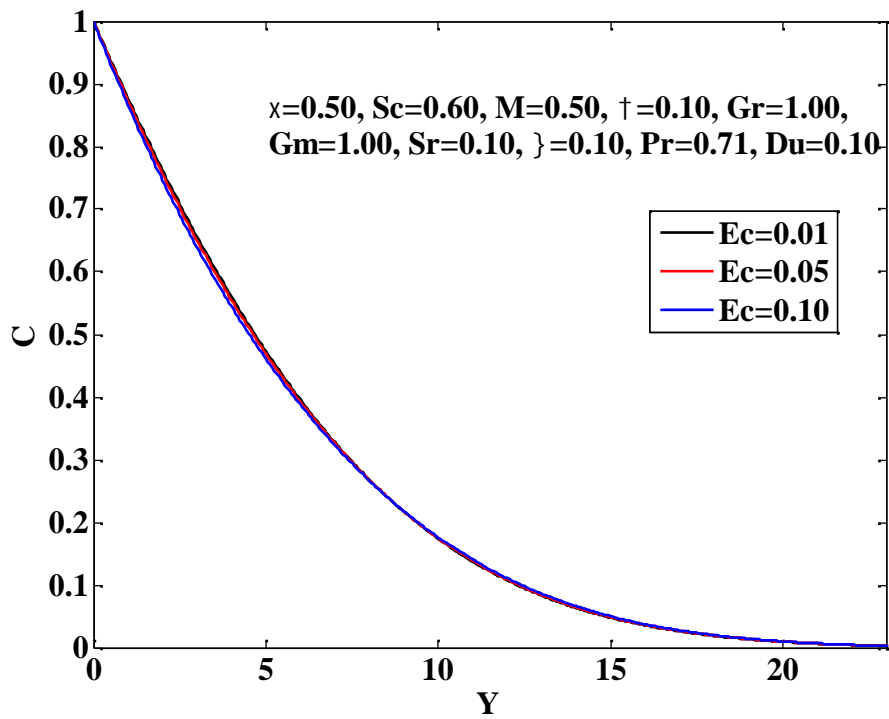


Figure 4.30: Velocity profiles for various values of Eckert Number,  $Ec$ .



**Figure 4.31:** Temperature profiles for various values of Eckert Number,  $Ec$ .



**Figure 4.32:** Concentration profiles for various values of Eckert Number,  $Ec$ .

The influence of variable thermal conductivity,  $\dagger$  on the velocity, temperature and concentration distributions are described in Figures 4.33 – 4.35. It is observed that velocity and temperature profiles are increased with the increase of  $\dagger$ . No effect of  $\dagger$  on the concentration distribution is observed here.

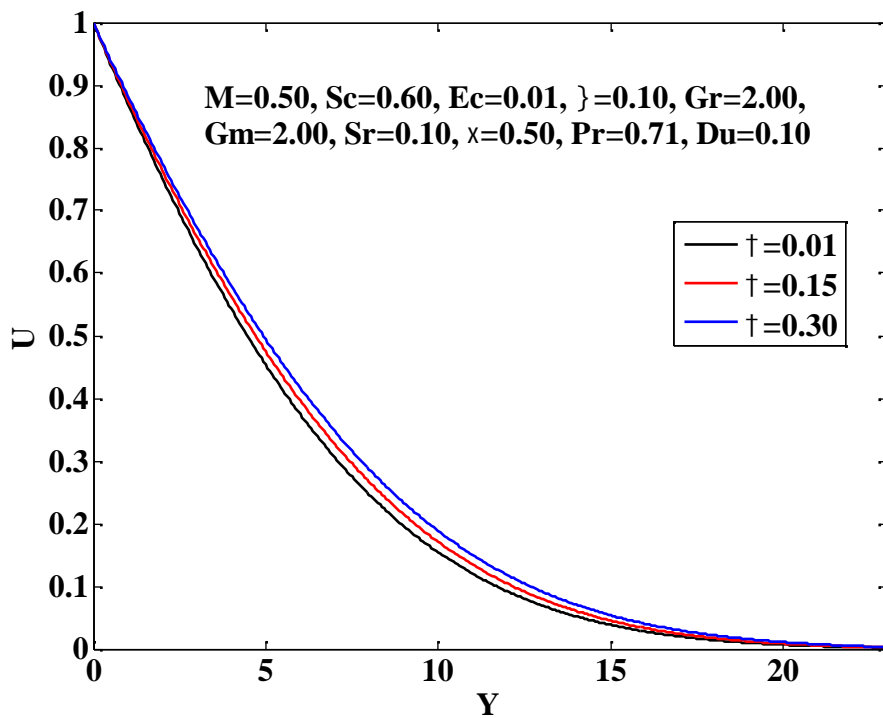


**Figure 4.33:** Velocity profiles for various values of Electrical Conductivity,  $\dagger$ .

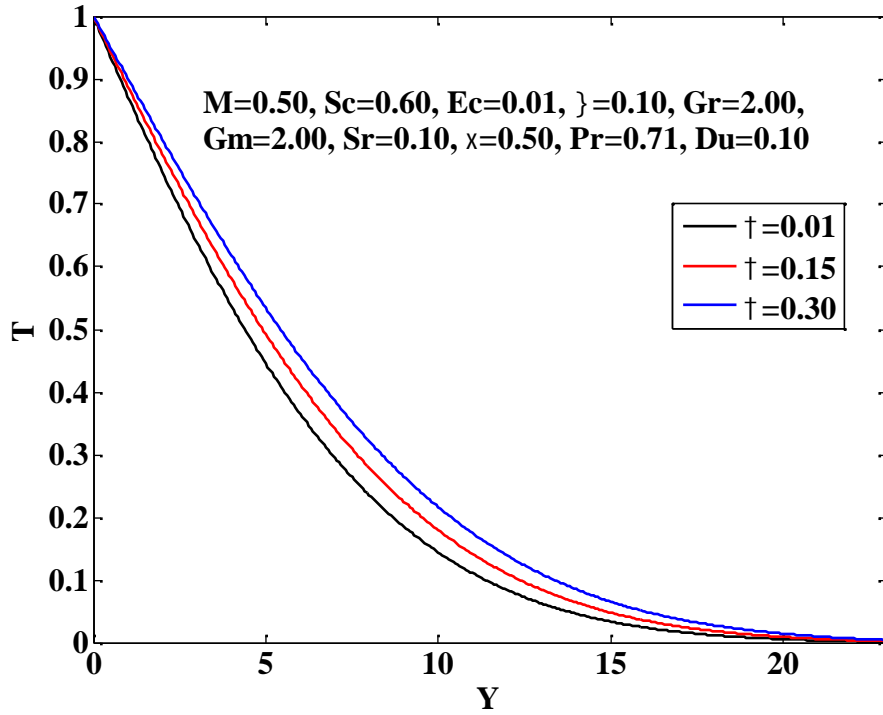


**Figure 4.34:** Temperature profiles for various values of Electrical conductivity,  $\dagger$ .

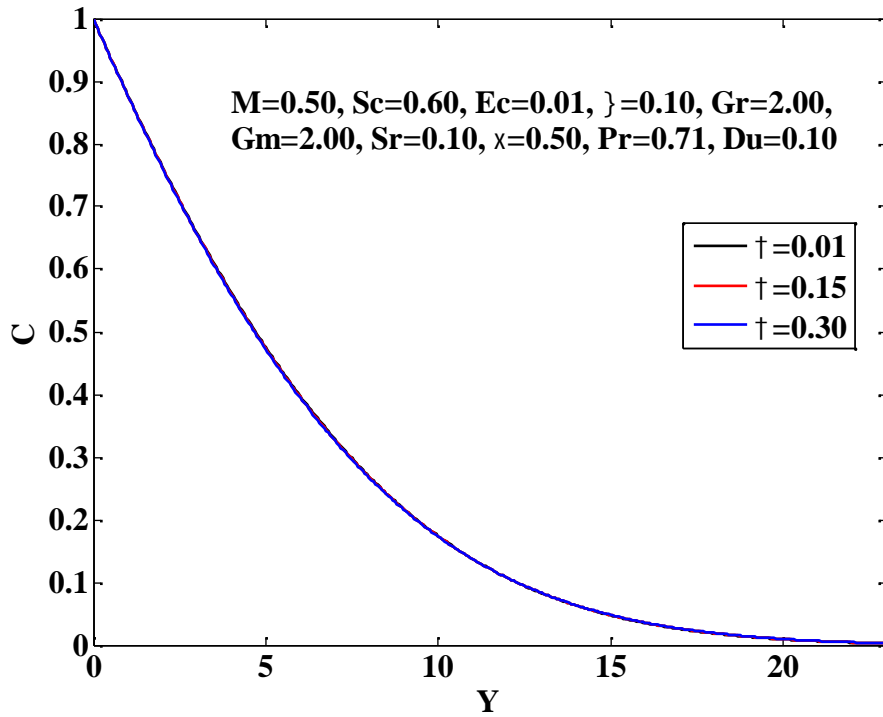


**Figure 4.35:** Concentration profiles for various values of Electrical conductivity,  $\dagger$ .

## REFERENCES

1. Alam, M. S. and Rahman, M. M. 1992, "Dufour and Soret effects on MHD free convective and mass transfer flow past a vertical flat plate embedded in a porous medium". *Journal of Naval Architecture and Marine Engineering*. 2(1): pp.369-374.
2. Alfvén, H., 1942, "On the existence of electromagnetic hydromagnetic waves", *F. Mat. Astro. Fysik .Bd.*, Vol. 2, pp.295.
3. Agrawal, H. L., Ram, P. C., and Singh, S. S., 1980, "Combined buoyancy effects of thermal and mass diffusion on MHD natural convection flows", *The Canadian Journal of Chemical Engineering*, Vol. 58(1), pp 131-133.
4. Alim, M. A., Alam, M. D. and Mamun, A., 2007, "Joule heating effect on the coupling of conduction with magneto hydrodynamic free convection flow from a vertical plate", *Non-Linear Analysis Modeling and Control*, vol. 12, no. 3, pp. 307–316.
5. Benjan, A., Dincer, I., Lorente, S., Miguel, A. F. and Reis, A. H., 2004, "Porous and complex flow structures in modern technologies", Springer, New York, NY.
6. Callahan, G. D. and Marner, W.J., 1976, "Transient free convection with mass transfer on an isothermal vertical flat plate", *International Journal of Heat and Mass Transfer*, Vol. 19(2), pp. 165-174.
7. Cowling, T. G. 1957, "Magnetohydrodynamics", *Interscience Publications*, New York.
8. Caldwell, D.R., 1974, "Experimental study on the onset of thermohaline convection", *J. Fluid Mech.*, Vol. 64, pp. 347-367.
9. Duwairi, H. M., 2005, "Viscous and Joule heating effects on forced convection flow from radiate isothermal porous surfaces", *International Journal of Numerical Methods for Heat and Fluid Flow*, vol. 15, no. 5, pp. 429–440.
10. De Groot, S. R., and Mazur, P., 1962, "Non-equilibrium thermodynamics", Interscience Publishers, New York, pp. 20.
11. Eckert, E. R. G. and Drake, R. M., 1974, "Analysis of Heat and Mass Transfer", McGraw-Hill, New York, NY, USA.
12. Faraday, M., 1832, "Experimental Researches in electricity", *Trans.* 15, 175.
13. Govardhan, K., Kishan, N. and Balaswamy, B., 2012, "Effect of viscous dissipation and radiation on MHD gas flow and heat and mass transfer over a stretching surface with a uniform free stream", *Journal of Engineering Physics and Thermophysics*, vol. 85, no. 4, pp. 909–916.
14. Hurle, D. T. J., and Jakeman, E., 1971, "Soret-driven thermosolutal convection", *Journal of Fluid Mechanics*, Vol. 47, pp. 667-687.
15. Ibrahim, S. M., 2013, "Effects of mass transfer, radiation, Joule heating and viscous dissipation on steady MHD Marangoni convection flow over a flat surface with suction and injection", *International Journal of Engineering Mathematics*,



- vol. 2013, Article ID903818, 9 pages.
16. Ingham, D. B. and Pop, I., 2005, "Transport phenomena in Porous media", Elsevier, Oxford, UK.
  17. Jai, S., 2012, "Viscous dissipation and chemical reaction effects on flow past a stretching surface in a porous medium", *Advance Theory of Applied Mechanics*, vol. 5, pp. 323–331.
  18. Jaluria, Y., 1980, "Natural convection heat and mass transfer", 5, *PergamonPress*, Oxford, UK.
  19. Kafousiasis, N. G, and Williams, E. M., 1995, "Thermal-diffusion and diffusion-Thermo effects on mixed free-forced convective and mass transfer boundary layer flow with temperature dependent viscosity", *International Journal of Engineering Science*, vol. 33, pp. 1369-1384.
  20. Khaleque, T. S. and Samad, M. A., 2010, "Effects of radiation, heat generation and viscous dissipation on MHD free convection flow along a stretching sheet", *Research Journal of Applied Sciences, Engineering and Technology*, vol. 2, no. 4, pp. 368–377.
  21. Levy, R. H., and Petschek, H. E., 1962, "LAS Paper", Los Angeles, California, June, pp. 62-100.
  22. Meyer, R. C., 1958, "On reducing aerodynamic heat transfer rates by magnetohydrodynamic techniques", *J. Aerospace Sci.* 25, pp. 561.
  23. Mansour, M. A., El-Anssary, N. F. and Aly, A. M., 2008, "Effect of chemical reaction and viscous dissipation on MHD natural convection flows saturated in porous media with suction or injection", *International Journal of Applied Mathematics and Mechanics*, vol. 4, no. 2, pp. 60–70.
  24. Mohammad, F., Masatiro, O., Abdus, S. and Mohamud, A., 2005, "Similarity solutions for MHD flow through vertical porous plate with suction", *Journal of Computational and Applied Mechanics*, vol. 6, no. 1, pp. 15–25.
  25. Makinde O. D., 2010, "On MHD heat and mass transfer over a moving vertical plate with a convective surface boundary condition", *The Canadian Journal of Chemical Engineering*, vol. 88, no. 6, pp. 983–990.
  26. Nield, D. A. and Bejan, A., 2006, "Convection in Porous media", Springer, New York, NY, USA, Third Edition.
  27. Patanker, S. V. and Spalding, D. V., 1970, "Heat and Mass transfer in Boundary Layer", 2<sup>nd</sup> Edition, *Interext Books*, London.
  28. Postelnicu, A., 2010, "Heat and mass transfer by natural convection at a stagnation point in a porous medium considering Soret and Dufour effects", *Heat and Mass Transfer*, vol. 46, no. 8-9, pp. 831–840.
  29. Palani, G. and Srikanth, U., 2009, "MHD flow past a semi-infinite vertical plate with mass transfer", *Nonlinear Analysis: Modelling and Control*, vol. 14, no. 3, pp. 345–356.
  30. Raptis, A. A. 1983, "Effects of mass transfer on the hydromagnetic flow past a vertical limiting surface", *Aatrophys. Space Sci.*, Vol. 92(1), pp. 135-142.
  31. Rossow, V. J., 1957, " On flow of electrically conducting fluids over a flat plate in the presence of transverse magnetic field", *NACA TN 3971*, pp. 1-54.
  32. Rosenberg, D. U. V., 1969, "Method of Numerical Solutions of Partial Differential Equations", *American Elsevier Pub. Co.*, New York.

33. Soundalgekar, V. M., and Ganesan, P., 1980, "Transient free convective flow past a semi-infinite vertical plate with mass transfer", *Reg. J. Energy Heat Mass Transfer*, Vol. 2(1), pp. 83-91.
34. Schlichting, H., 1968, "Boundary Layer theory", McGraw-Hill, New York.
35. Sutton, G. W., and Gloersen, P., 1961 "2nd Symposium on the Engineering Aspects of MAGNETOHYDRODYNAMICS", *Physics Today*, Vol. 14(9), pp. 18.
36. Sarada, K. and Shankar, B., 2013, "The effects of Soret and Dufour on an unsteady MHD free convection flow past a vertical porous plate in the presence of suction or injection", *International Journal of Engineering and Science*, vol. 2, no. 7, pp. 13–25.
37. Sattar, M. A., 1993, "Free and forced convection boundary layer flow through a porous medium with large suction", *International Journal of Energy Research*, vol. 17, no. 1, pp. 1–7.
38. Uwanta I. J. and Usman, H., 2014, "On the Influence of Soret and Dufour Effects on MHD Free Convective Heat and Mass Transfer Flow over a Vertical Channel with Constant Suction and Viscous Dissipation", Hindawi Publishing Corporation, *International Scholarly Research Notices*, Volume 2014, Article ID 639159, 11 pages, <http://dx.doi.org/10.1155/2014/639159>
39. Usman, H. and Uwanta, I. J., 2013, "Effect of thermal conductivity on MHD Heat and Mass transfer: flow past an infinite vertical plate with Soret and Dufour effects", *American Journal of Applied Mathematics*, vol. 1, no. 3, pp. 28–38.
40. Uwanta, I. J., Asogwa, K. K. and Ali, U. A., 2008, "MHD fluid flow over a vertical plate with Dufour and Soret effects", *International Journal of Computer Applications*, vol. 45, no. 2, pp. 8–16.
41. Uwanta, I. J., 2012, "Effects of chemical reaction and radiation on Heat and Mass Transfer past a semi-infinite vertical porous plate with constant mass flux and dissipation", *European Journal of Scientific Research*, vol. 87, no. 2, pp. 190–200.
42. Vafai, K., 2005, "Hand book of porous media", Second edition. Taylor and Francis: New York.